Supercapacitors Performance Evaluation

*Sanliang Zhang and Ning Pan**

The performance of a supercapacitor can be characterized by a series of key parameters, including the cell capacitance, operating voltage, equivalent series resistance, power density, energy density, and time constant. To accurately measure these parameters, a variety of methods have been proposed and are used in academia and industry. As a result, some confusion has been caused due to the inconsistencies between different evaluation methods and practices. Such confusion hinders effective communication of new research findings, and creates a hurdle in transferring novel supercapacitor technologies from research labs to commercial applications. Based on public sources, this article is an attempt to inventory, critique and hopefully streamline the commonly used instruments, key performance metrics, calculation methods, and major affecting factors for supercapacitor performance evaluation. Thereafter the primary sources of inconsistencies are identified and possible solutions are suggested, with emphasis on device performance vs. material properties and the rate dependency of supercapacitors. We hope, by using reliable, intrinsic, and comparable parameters produced, the existing inconsistencies and confusion can be largely eliminated so as to facilitate further progress in the field.

1. Introduction

The detrimental long-term effects of greenhouse gas emission into the atmosphere and the finite supply of fossil fuels underscore the urgency of exploring renewable energy resources and the related energy generation, storage, and conservation technologies. A major hurdle, in general, lies in the dependence on the power line for electricity supply. The proposed wireless power supply[1,2] is still largely in the exploration stage and is unlikely to play a significant role in foreseeable future. The pending obstacle for the use of renewable energy from wind and solar sources is the stability and quality of the produced electricity.[3] Driven by such need for power storage, rectification, transport, and supply on various scales, sustained and extensive research and exploration have been conducted, and a number of electrical energy storage (EES) technologies have been developed so far; some are in use in our daily lives, such as batteries and fuel cells, and others are more for industrial applications, including pumped hydro, flywheel, compressed air, superconducting magnetic, and supercapacitors.[4]

Of these EES technologies, batteries have been widely used on various scales and have been continuously studied due to their outstanding performance. Based on the specific battery chemistry, they can be rechargeable or non-rechargeable. Both produce electricity from chemical energy via redox reactions at the anode and cathode. For rechargeable batteries, they can reverse this process for certain times.[5–7] Beginning in 20th century, batteries have become increasingly ingrained in our daily life. However, there are certain areas where batteries revealed shortcomings or failed to meet the needs, including: 1) Low power density: This issue has severely hindered applications where high power discharge and/or recharge rate are required. 2) Heat generation: The redox reactions in batteries may lead to Joule heating and thermochemical heating during their operation.[8,9] Such heat, if not dissipated, will effectively result in overheating, thermal runaway, and even fire.[10] 3) Limited cycle life: The cycle lives of batteries are normally limited due to the lack of fully reversible redox reaction during the discharge and recharge process.[5]

Because of the issues listed above, batteries alone are unable to provide the full solution for electricity storage. A durable and safe electricity storage device, with high power and/or energy performance, will undoubtedly transform the landscape of electric energy generation, distribution, and utility. Additionally, as consumer, industry, and military applications require more compact and reliable electrical power systems, the development of such devices continues to be one of the major thrusts in the area.[11–13]

1.1. Supercapacitors and the Charge Storage Mechanisms

Supercapacitors (SCs), often referred to as ultracapacitors or electrochemical capacitors, demonstrate outstanding power performance, excellent reversibility, very long cycle life (>1 000 000 cycles), simple mode of operation, and ease of integration into electronics.[14–22] In addition, they generate less thermochemical heat because of the simpler charge storage mechanisms associated.[23] Therefore, they have been widely used in consumer electronics, memory back-up systems, and industrial power and energy management[5,14] and will be found in more niche markets in the near future.[24]

S. Zhang, Prof. N. Pan
Department of Biological and Agricultural Engineering
University of California at Davis
Davis, CA 95616, USA
E-mail: npan@ucdavis.edu

DOI: 10.1002/aenm.201401401

1.1.1. Charge Storage Mechanisms

It is generally accepted that there are two charge storage mechanisms involved in the operation of SCs: a) electrostatically storing the charges at the interface of capacitor electrode as electric double layer capacitance and b) faradaically storing the charges at the electrode surface as pseudocapacitance.[25]

Electric double layer (EDL) refers to the two charged layers formed at theelectrode/electrolyte interfaces[26] and the resulting potential-dependent charge storage ability is ascribed to electric double layer capacitance. The earliest model of EDL is usually attributed to Helmholtz[27,28] and thus EDL is also referred to as Helmholtz double-layers. Later, the Gouy–Chapman model and the Gouy–Chapman-Stern model were developed to more accurately describe the detailed structure of EDLs.[26,29]

Electricity storage and delivery via EDL was first proposed by Becker in 1957 (U.S. Patent 2 800 616),[30] and the resulting SCs are then called electric double layer capacitors (EDLCs). High-surface-area activated carbon (AC) is normally used in the system as the working medium. Because of their huge surface area, EDLCs can store much more electricity and are usually evaluated in Farads (F), whereas conventional dielectric and electrolytic capacitors are evaluated in picofarads (pF) and microfarads (μF).

Pseudocapacitance arises at the electrode surfaces where the charges are faradaically stored. Stemming from thermodynamic reasons, the faradaic charge transfer process across the electric double layer leads to a special potential-dependent charge accumulation or release phenomenon such that the derivative dq/dV is equivalent to a capacitance.[31] It is manifested by the triangular shape of charge/discharge curves at constant current density and the rectangular shape of cyclic voltammograms for pseudocapacitors (PCs).[32] Such faradaic charge transfer process was introduced by Trasatti et al.,[33] attributed to the highly reversible surface redox reaction.[34] Normally during charging, the surface region of redox-active electrode materials, i.e., RuO_2, Mo_xN or MnO_2,[35–38] are reduced to lower oxidation states coupled with adsorption/insertion of cations from the electrolyte at/near the electrode surfaces. Upon discharge, the process can be almost fully reversed.

1.1.2. Overall Charge Storage Ability and Hybrid Capacitors

In practice, the overall charge ability of a SC is enabled by both of the two charge storage mechanisms. They coexist in SCs and contribute in different proportions. For example, the charge storage of AC-based EDLCs is dominated by the formation of EDLs, but the oxygen-containing groups on AC surface may induce some surface redox reactions.

Furthermore, hybrid capacitors (HCs) made by combining various capacitive electrodes from EDLCs and/or PCs with battery electrodes have been reported so as to improve the energy storage ability while maintaining the high power performance.[39–41] The most widely acknowledged hybrid system is the Li-ion capacitor (LIC), which is normally produced by using $Li_4Ti_5O_{12}$ nanocrystals[42–44] or advanced graphite materials[45,46] as the positive electrode and AC as the negative electrode. The charge storage is realized by Li^+ intercalation. More recently, a family of 2D carbides and carbonitrides have also been investigated for the similar purpose by single- or multivalent cation intercalation.[47] By coupling $Ni(OH)_2$ electrode and EDLC electrode, JSC ESMA from Russia has commercialized the resulting hybrid capacitor with the capacitance from 3 to 8 kF.[48] Another example called the "ultrabattery" is based on the combination of a lead-acid battery and EDLC.[49–52] The combination of high energy density of batteries materials with long cycle life and short charging time of supercapacitors materials is considered a very promising direction. More detailed descriptions of these hybrid devices have been published previously.[53]

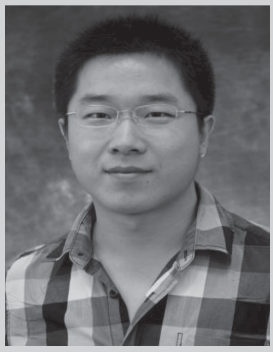

Sanliang Zhang received his B. Eng. degree in textile engineering from Donghua University, Shanghai, in 2011. He is now a Ph.D. candidate in Biological Systems Engineering working with Prof. Dr. Ning Pan at the University of California, Davis. His current research focuses on novel electrode fabrication, advanced 2D nanostructural materials, supercapacitor performance evaluation, and charge storage mechanism analysis.

Ning Pan is a professor of Biological Systems Engineering at the University of California, Davis. His research interests include soft fibrous materials, nanoscale energy materials and biomechanics. He received his B. Eng. from NW University of Engineering, and PhD from Donghua University in China, and postdoc at MIT.

1.2. Performance Evaluation for Supercapacitors

To evaluate SCs performance, three essential parameters, cell (total) capacitance C_T, operating voltage V_o, and equivalent series resistance R_{ES}, are often used to assess their energy and power performance, and usually are sufficient for commercial products where the materials, fabrication, and cell design are all fixed. However, in the research arena of constant probing for novel materials, more advanced manufacturing processes, and new cell designs, additional factors become indispensible. In fact, there is a rather large group of important factors necessary to paint the whole picture for supercapacitors and an overview of the complex interrelationship between the different performance metrics, the major affecting factors, and the corresponding test methods is presented in **Figure 1**. Several color schemes are employed

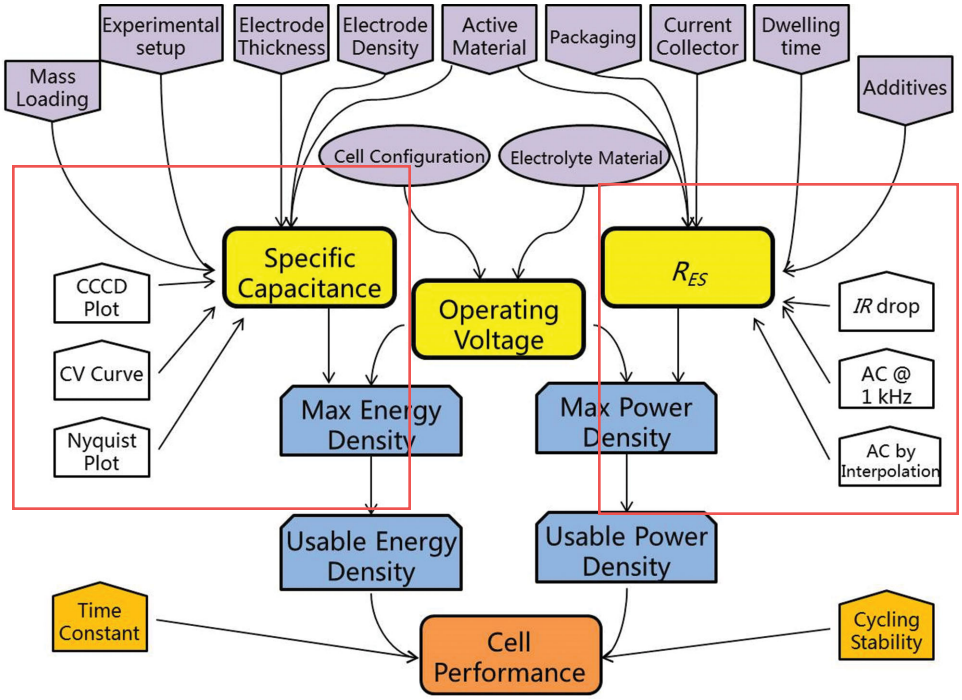

Figure 1. An illustration of key performance metrics, test methods, major affecting factors for the evaluation of SCs.

in the figure: the three core parameters are highlighted in yellow; the power and energy densities in dark blue; time constant and cycling stability in light orange; all the important affecting factors in light purple; and the corresponding test methods in white. The figure is for illustration purpose and is by no means exclusive in presenting all the factors or detailing the complex multifaceted connections between them. For example, the evaluation method for V_o and the influence of electrolyte materials on specific capacitance are not explicitly presented.

Giving the multiple performance metrics, test methods, and affecting factors shown in Figure 1, and the multifaceted relationships among them, inconsistencies become inevitable in the test results for the same cell measured in different labs, using different methods, and between academia and industry. To understand the causes for such inconsistencies, some important issues have to be addressed, including material property vs. device performance and the rate dependency of supercapacitor performance.

Many attempts have been carried out to standardize the evaluation methods for SC devices. Some national and international bodies including DOD (US Department of Defense), DOE (US Department of Energy), IEC (International Electrochemical Commission), and SAE (Society of Automotive Engineers) have worked intensively on this matter. The resulting documents are summarized chronologically in **Table 1**.

Apparently, such efforts are mainly for specific applications oriented for industry, and there is still lacking a general understanding and knowledge collected/derived from the most recent cutting edge research so as to guide a more accurate and effective practice for performance evaluation of SCs. This prompts our intention in writing this article.

In view of the urgent need for more reliable test methods called for by the drastic pace in searching for new energy storage solutions, and the complexities involved, this article represents an attempt to clarify and streamline the existing evaluation methods, in the hopes of eliminating or at least alleviating such inconsistencies, and to facilitate more effective communication in the field.

Table 1. A chronological review of SC evaluation standards.

Year	Organization	Title	Document ID
1986	DOD	Capacitors, fixed, electrolytic, double layer, carbon (metric), general specifications	DOD-C-29501
1994	DOE	Electric vehicle capacitor test procedures manual	DOE/ID-10491
2004	DOE	FreedomCAR ultracapacitor test manual	DOE/NE-ID-11173
2006	IEC	Fixed electric double layer capacitor for use in electronic equipment	IEC 62391
2009	IEC	Electric double layer capacitors for use in hybrid electric vehicles – Test methods for electrical characteristics	IEC 62576
2012	IEC	Railway applications – Rolling stock equipment – Capacitors for power electronics – Part 3: Electric double-layer capacitors	IEC 61881–3
2013	SAE	Capacitive energy storage device requirements for automotive propulsion applications	J3051

2. Instruments and Measurements of Key Metrics

2.1. Instruments

Various instruments or test modes have been developed and applied to characterize the electrochemical performance of SCs. Cyclic voltammetry (CV), constant current charge/discharge (CCCD), and electrochemical impedance spectroscopy (EIS) tests are commonly used. In essence, all such instruments can be used to measure the three fundamental parameters: voltage, current, and time; other metrics, including the capacitance, equivalent series resistance, operating voltage, and, subsequently, the time constant, energy, and power performance of SCs, can be derived from them. However, each of the instruments has its own focus and targeted parameters, by design, and their applications and limits are discussed below.

In addition, the three test modes can be used to examine SC materials, i.e., the electricity storage media including electrode materials and electrolyte materials, and SC devices, i.e., the whole package of SCs. Clear differentiation between a property measured for the cell or just for its active material has to be made when reporting a test result; this is a clearly logical practice yet it is often ignored. Additionally, technical differences exist when testing SC devices versus SC materials and we will stress this in our discussion.

2.1.1. Cyclic Voltammetry (CV)

CV testing applies a linearly changed electric potential between positive and negative electrodes for two-electrode systems, or between reference and working electrodes for three-electrode configurations. The speed of the potential change in mV s^{-1} is designated as the sweep rate or scan rate, v, and the range of potential change is called the potential window or operating potential. The instantaneous current during the cathodic and anodic sweeps is recorded to characterize the electrochemical reactions involved. The data are plotted as current (A) vs. potential (V) or sometimes as current (A) or potential (V) vs. time (s).[29]

To examine the charge storage mechanisms of SC materials where EDLC and PC types are separate, CV testing with the three-electrode setup is regarded as the most suitable approach.[34,35] The test results can first be analyzed by examining the shape of the CV curves, as for EDLC and most PC materials, the shape of the resulting CV curves is rather rectangular, whereas for some PC materials, pronounced redox peaks may occur in a highly reversible manner.[32] Therefore, it is not sufficient to differentiate EDLC and PC materials by solely observing the shape of CV curves.

A more quantitative and reliable method for interpreting the data from a CV test to extract the contributions from EDL and PC mechanisms separately is by utilizing the knowledge that the instantaneous current induced by the EDL mechanism is proportional to the scan rate, while the semi-infinite diffusion limited cation adsorption/insertion at/near the electrode surface from PC mechanism is proportional to the square root of the scan rate.[38,54–60] However, this approach is limited in its ability to separate the contribution of surface-redox reactions from EDL mechanisms due to the fact that they happen roughly on the same time scale.[29] Therefore, more experimental and theoretical studies are required to address this issue.

CV testing is also suitable in practice to determining the operating voltage or potential window for SC materials by successive adjustment of the reversal potential in a three-electrode system, and the reversibility of the charge and discharge processes can also be studied simultaneously.[31,38] In addition, the specific capacitance and energy performance of the SC materials can be obtained via integration of the CV curves as discussed in detail later. Similar process can also be conducted for SC devices to obtain their total cell capacitance and hence the amount of electricity stored.

2.1.2. Constant Current Charge/Discharge (CCCD)

CCCD testing is the most widely used method for the characterization of SCs under direct current.[25,61] It is conducted by repetitive charging and discharging of the SC device or the working electrode at a constant current level with or without a dwelling period (a time period between charging and discharging while the peak voltage V_o remains constant), and normally a plot of the potential (E) vs. time (s) is the output. Choosing a proper level of the constant current is critical to produce consistent and comparable data from a CCCD test.

CCCD test is regarded as the most versatile and accurate approach in characterizing SC devices. All three core parameters of SC devices, C_T, R_{ES}, and V_o, can be tested from it and subsequently used to derive most of the other properties, such as the time constant, power and energy densities, and leakage and peak current. It can also be conveniently used to study the cycling stability of SC devices. Moreover, by using a three-electrode setup, the specific capacitance, reversibility, and potential window for SC materials can also be obtained via CCCD test.

2.1.3. Electrochemical Impedance Spectroscopy (EIS)

EIS testing, also known as the dielectric spectroscopic testing, measures the impedance of a power cell as a function of frequency by applying a low-amplitude alternative voltage (normally 5 mV) superimposed on a steady-state potential. The resulting data are usually expressed graphically in a Bode plot to demonstrate the cell response between the phase angle and frequency, and in a Nyquist plot to show the imaginary and real parts of the cell impedances on a complex plane.[62,63]

In addition to the frequency response and impedance, EIS has also been used to characterize the charge transfer, mass transport, and charge storage mechanisms, as well as to estimate the capacitance, energy, and power properties.[64,65] Different equivalent circuits and models have been developed to distinguish the contribution of individual structure component in a cell system to the total impedance.[45,66,67] When SC devices are tested, the real parts of the complex impedance at selected frequencies are used in literature to represent R_{ES}. However, one needs to keep in mind that this R_{ES} from an EIS test is

often much smaller than that derived from the CCCD test,[68] and is therefore limited in describing the power performance of SC devices.

For SC materials, EIS testing can be used to study the impedance, specific capacitance, charge transfer, mass transport, and charge storage mechanisms involved by executing similar analysis in a three-electrode system.

2.2. Capacitance

The total capacitance C_T of a SC is a reflection of the electrical charge ΔQ stored under a given voltage change ΔV:

$$C_T = \frac{\Delta Q}{\Delta V} \quad (1)$$

This is preferred when specifying the total charge storage ability of SC devices. A more intrinsic specific capacitance C_S is defined to measure, preferably, the charge storage ability of SC materials:

$$C_s = \frac{\Delta Q}{\Delta V \Pi} \quad (2)$$

where Π can be the mass, volume, surface area of the electrode material, or even the size of the electrode, and the resulting specific capacitance C_S is often named correspondingly as the gravimetric capacitance (F g^{-1}), volumetric capacitance (F mL^{-1}), normalized capacitance (μF cm^{-2}) and areal capacitance (F cm^{-2}) or linear capacitance (F cm^{-1}). Sometimes, C_S is also used to describe device performance, when normalized by the whole cell weight or volume.[69] Note that although C_S is considered the most important parameter in comparing the charge storage ability of SC materials, it is rarely mentioned by industry, as most of the commercial SCs are activated carbon (AC) based, and its C_S is generally considered a constant between 100 F g^{-1} and 70 F cm^{-3} in organic electrolyte.[70] However, for scientists searching for new materials, C_S is the more informative way to depict the charge storage ability of a given material.

2.2.1. Evaluation of C_T

The total capacitance C_T of a cell in Equation (1) can be further expressed as:

$$C_T = \frac{\Delta Q}{\Delta V} = \frac{\int_0^{2V_o/v} |i|\,dt}{2V_o} \quad (3)$$

Through the integration of the resulting cyclic voltammograms, the accumulated charge as a function of potential can be obtained. Normally, the whole curve is recommended to for use,[71–75] as shown in Equation (3). However, in practice, different segments of the curve, as depicted in **Figure 2** in distinct colors, have been used in integration,[76–79] thus leading to inconsistencies in test results.[73,74,77,80–82] It is worthy noting that the potential change in Equation (3) $\Delta V = 2V_o$ (0 to V_o and back to 0), for there are mistakes made in ΔV values.[83–86]

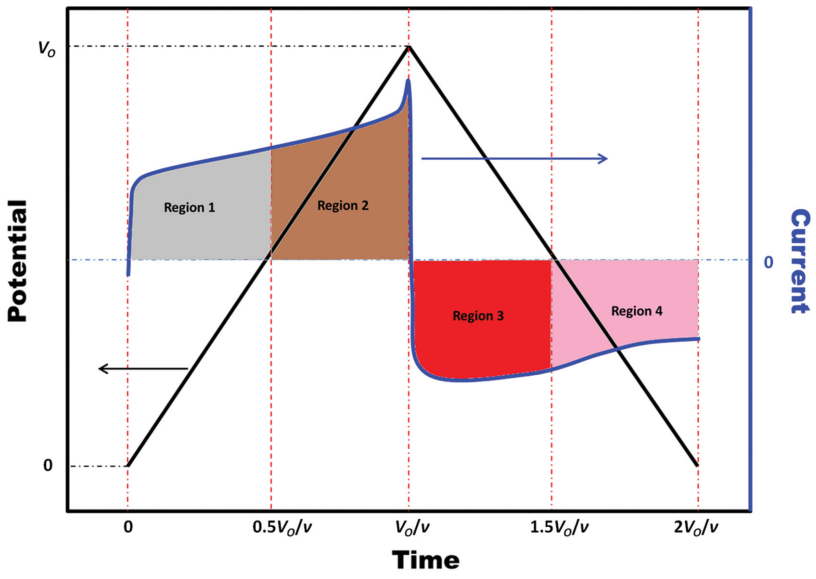

Figure 2. An illustration of a typical CV test result.

Because constant current is used in a CCCD test, Equation (1) can be converted to:

$$C_T = \frac{I\Delta t}{\Delta V} \quad (4)$$

where I is the constant current, Δt is the charging or discharging time corresponding to the specified potential change ΔV. So the key issue now is that the correct time Δt and ΔV are used in calculation. Often the entire discharging curve is used:

$$C_T = \frac{I_{dis}\Delta t_{Vo-2Vo}}{V_o} \quad (5)$$

Since IR drop is inevitable in CCCD test, one can adjust ΔV so as to exclude the IR drop for more accurate result, i.e.,

$$C_T = \frac{I_{dis}\Delta t_{V_o-2V_o}}{V_o - V_{IR\text{-}drop}} \quad (6)$$

Similar to CV tests, different segments of the CCCD plots, illustrated in **Figure 3**, have been used in computing the cell capacitance.[74,79,87] This time, because the current remains constant, an identical C_T value is obtained independent of the segment used, as long as the voltage changes linearly with time as in Figure 3.

For hybrid capacitors (HCs) (mainly $Ni(OH)_2$ or PbO_2 based[61,70,88] with nonlinear curves as seen in **Figure 4**, the selection of different regions from the curve can make a large

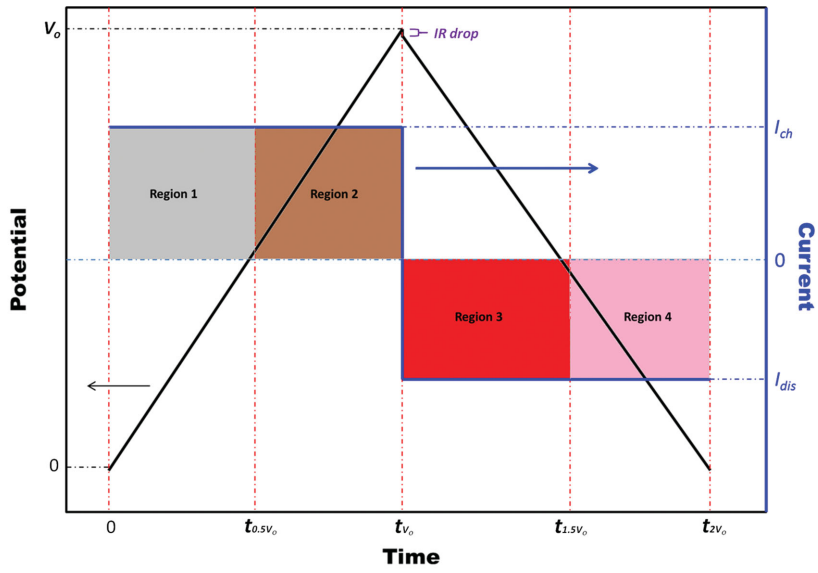

Figure 3. An illustration of CCCD test result from EDLCs or PCs with linear potential change over time.

difference in determining ΔV, and hence C_T.[89–92] In such cases, the use of a proper or fixed region, or the selection of suitable potential window, becomes critical and needs to be standardized. Based on work by Burke,[61] Region 3 or a potential window from V_o to the shoulder voltage is recommended. Likewise, one can also adjust ΔV to eliminate the IR drop to improve accuracy.

The conventional method of deriving capacitance from EIS test is based on the imaginary part of the complex impedance Im(Z) as shown in Equation (7):[7,62,93]

$$C_{Tf} = -\frac{1}{2\pi f \mathrm{Im}(Z)} \tag{7}$$

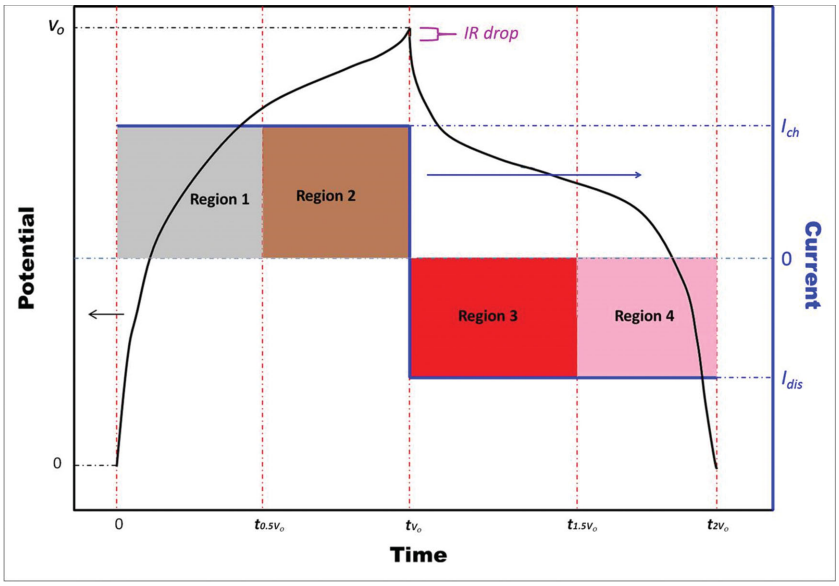

Figure 4. An illustration of CCCD test result from HCs with nonlinear potential change over time.

where f is the frequency. Normally this frequency is identified at which the phase angle reaches –45 degrees,[93] or simply as the lowest frequency applied.[7]

Another method introduced by Simon et al. is:[64]

$$\mathrm{Re}(C) = \frac{-\mathrm{Im}(Z)}{\omega |Z|^2} \tag{8}$$

$$\mathrm{Im}(C) = \frac{\mathrm{Re}(Z)}{\omega |Z|^2} \tag{9}$$

where $Z = \sqrt{\mathrm{Re}(Z)^2 + \mathrm{Im}(Z)^2}$ is the overall complex impedance, $\omega = 2\pi f$ is angular velocity, Re(Z) is the real part of the complex impedance, and Re(C) and Im(C) are the real and imaginary capacitances, respectively. Im(C) is a term related to the energy dissipation of the cell, and Re(C), calculated at the lowest-frequency applied, indicates the energy stored, thus can be used to represent C_T.[64]

2.2.2. Evaluation of C_S

Once C_T is obtained, the corresponding C_S can be calculated using Equation (4). This seemingly straightforward step is made complicated by the fact that there is no established standard procedure in determining the base value for Π, be the mass, volume, or other quantity. A mediocre C_T value can lead to an excellent C_S if a sufficiently small Π is used. For this reason, along with other possible considerations, technical or cost related, although attractive C_S results are frequently reported,[83–86,89–92] few have been successfully transferred to commercial products. One solution to this problem is that both C_T and the corresponding C_S values, as well as the Π value, be explicitly reported side by side. In addition to Π, other factors, as discussed in next section, including experimental setup, mass loading, and electrode thickness, and electrode density, can also alter the C_S value dramatically[73,94,95] and therefore recommended to be reported as necessary information.

2.2.3. Major Affecting Factors

Studies have demonstrated that quite different C_S values can be obtained for the same SC electrode when different experimental setups are adopted.[77] The three major experimental setups: symmetric two-electrode, asymmetric two-electrode, and three-electrode configurations, are

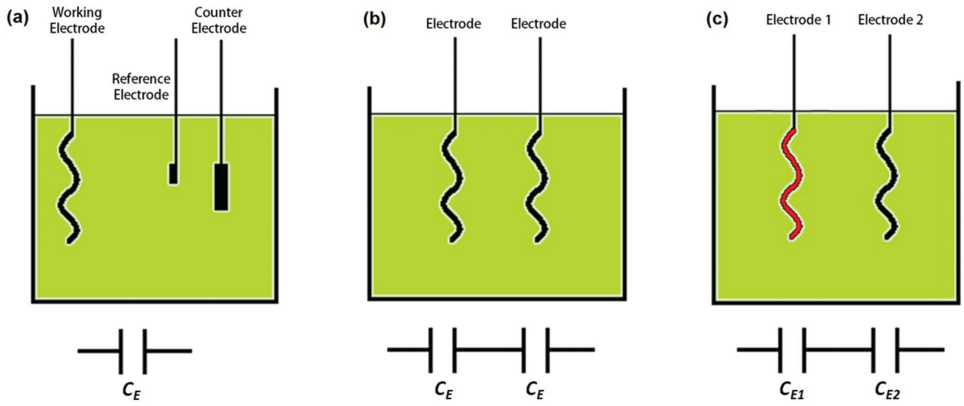

Figure 5. Schematic illustrations and equivalent circuits for different experimental setups.

illustrated in **Figure 5**. The three-electrode one is particularly useful in accurately determining the C_S for SC materials, and the two-electrode ones are normally used in SC device prototypes or final products. It is worth noting that it is also possible[96] to insert a reference electrode in the two-electrode system to study the detailed potential change in other two electrodes, but this scenario is not included here, and the three-electrode configuration mentioned in this article solely refers to the setup presented in Figure 5a.

The following analysis demonstrates how different setups can lead to different results. For brevity the gravimetric C_S is used. The weight of each individual electrode in Figure 5a,b is assumed to be m, while m_1 and m_2 are for the two different Electrodes 1 and 2 in Figure 5c. Assigning the single electrode capacitance as C_E, the gravimetric C_{Sa} in the three-electrode system can be calculated as:[67]

$$C_{Sa} = \frac{C_E}{m} \tag{10}$$

For the symmetric two-electrode system shown in Figure 5b, the cell total capacitance C_{Tb} can be obtained using:

$$\frac{1}{C_{Tb}} = \frac{1}{C_E} + \frac{1}{C_E} \tag{11}$$

By counting the mass for both electrodes, hence:

$$C_{Sb} = \frac{C_{Tb}}{2m} = \frac{1C_E}{4m} \tag{12}$$

That is, even with identical SC material, the specific capacitance obtained from the three-electrode system actually quadruples that from the symmetric two-electrode system, i.e.,

$$C_{Sa} = 4C_{Sb} \tag{13}$$

This relationship has been validated experimentally by Béguin et al.[77]

For the asymmetric two-electrode system in Figure 5c, the cell capacitance C_{Tc}:

$$\frac{1}{C_{Tc}} = \frac{1}{C_{E1}} + \frac{1}{C_{E2}} \tag{14}$$

Again by counting the mass for both electrodes, there is:

$$C_{Sc} = \frac{C_{Tc}}{m_1 + m_2} = \frac{1}{m_1 + m_2}\frac{C_{E1}C_{E2}}{C_{E1} + C_{E2}} \tag{15}$$

In this configuration, the electrode capacitances of the two electrodes are balanced to fully unitize the charge storage ability of the SC material, i.e., $C_{E1} = C_{E2} = C_E$. By using other active materials, such as pseudocapacitive ones, it is normally accepted that the specific capacitance of Electrode 1 is larger. Conversely if the two electrodes achieve the same capacitance C_E, then less mass is needed in Electrode 1, say at a fraction α ($0 < \alpha < 1$) of Electrode 2, so that $m_1 = \alpha m$, $m_2 = m$. Substituting them into Equation (15) yields,

$$C_{Sc} = \frac{1}{2(1+\alpha)}\frac{C_E}{m} \tag{16}$$

Combined with Equation (10) and (12), there are:

$$C_{Sa} = 2(1+\alpha)C_{Sc} \tag{17}$$

and

$$C_{Sb} = \frac{(1+\alpha)}{2}C_{Sc} \tag{18}$$

Thus the three equations show distinctive results when using setup a, b, or c. For example, if the specific capacitance in Electrode 1 doubles that in Electrode 2, $\alpha = 0.5$ at the same potential window. Then there is $C_{Sa} = 3C_{Sc}$ and $C_{Sb} = 0.75C_{Sc}$.

It is worth noting that for SC devices, the total capacitances for symmetric and asymmetric are identical under the same assumptions:

$$C_{Tb} = C_{Tc} = \frac{1}{2}C_E \tag{19}$$

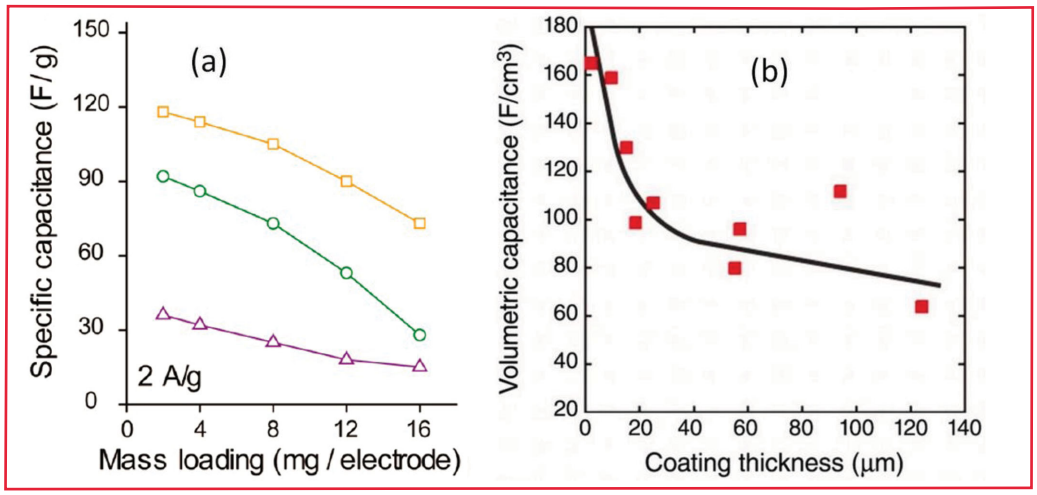

Figure 6. a) Effect of mass loading and b) electrode thickness on the resulting C_S: yellow squares, green circles and purple triangles represent crumpled graphene balls, wrinkled graphene sheets, and flat graphene sheets as electrodes; and red solid squares indicate carbide-derived carbons (CDCs) as electrodes. Panel (a) reproduced with permission.[107] Copyright 2013, American Chemical Society. Panel (b) reproduced with permission.[95] Copyright 2010, The American Association for the Advancement of Science.

The advantages of using asymmetric systems include first, as discussed below in 2.4.2, by using asymmetric system, additional electrochemical potential difference can be introduced so that the operating voltage of the cell can be boosted.[81] The second benefit is that for the same total capacitance, in an asymmetric system, the electrode of better PC material can cut the material use by a fraction $(1 - \alpha)$ as demonstrated above. This can be significant if this PC material is so superior that α is small. However so far, the symmetric SC devices still demonstrate better power performance, and consequently play a dominant role in the market, despite the intensive study on asymmetric systems.[81,90,97–102]

Mass loading is defined as the mass of active material per unit area of the electrode, and electrode thickness is the net thickness of the active material on the current collector. These two parameters reflecting the fabrication process significantly impact the resulting C_S, but are often not specified. Many studies used a very small mass loading or electrode thickness in calculating the specific capacitance C_S, and the resulted C_S appears outstanding in number but is often not meaningful in practice.[103,104] In general, it is suggested[73] that the mass loading to be at least 5 mg cm^{-2} and the electrode thickness between 50–200 μm. Exceptions may be found for micro-SCs [95,105,106] in special applications. **Figure 6**a,b are two verifications showing the significant impact of them on C_S.

The electrode density describes how densely the electrode materials are packed on current collector, and is expressed in mass/volume. Although it is related to both mass loading and electrode thickness, there is the material density involved. It is reported that the same electrode material with different packing densities can significantly influence the resulting electrochemical performance, including C_S, energy and power densities. Based on the targeted applications, there is an optimal level for the electrode density, so that the electrode is not over densely packed as to reduce the accessibility of SC materials, nor is it excessively loose to affect the volumetric performance. An example of its impact is provided in **Figure 7** by using certain graphene materials with increasing densities from 0.13 to 1.33 g cm^{-3}.[69]

2.3. Equivalent Series Resistance

A SC is not an ideal electrical component in the sense that it has its own internal resistance, and thus dissipates the energy that is stored. A SC cell can be simply treated as a system of a capacitor in series arrangement with a resistor R_{ES}, as shown in **Figure 8**. The resistance of this resistor is usually called the equivalent series resistance, R_{ES}, and is essential in reflecting the power performance and energy efficiency of SCs. In general, a small R_{ES} is preferred for better electrochemical performance and it can be normalized by the footprint area of one

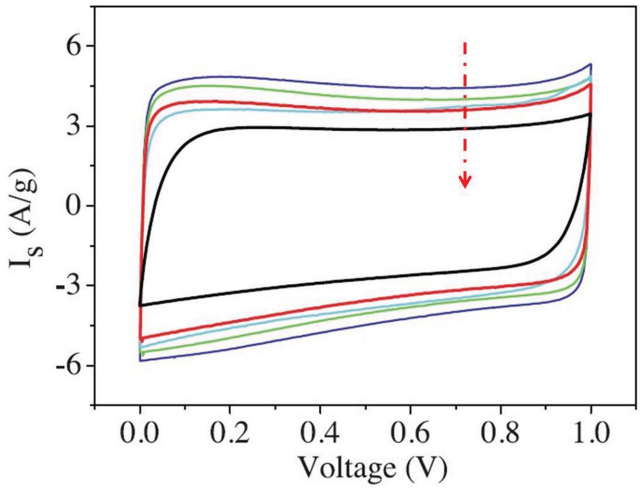

Figure 7. Cyclic voltammograms of liquid-mediated graphene materials with increasing electrode density from 0.13 to 1.33 g cm^{-3} following the dashed red arrow. Reproduced with permission.[69] Copyright 2014, The American Association for the Advancement of Science.

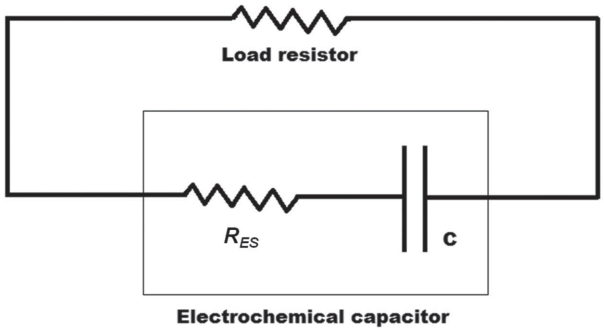

Figure 8. The series RC circuit for supercapacitors.

electrode as in Ω cm^{-2} for comparison. Note that in actual measurements, only a packed cell can give an accurate R_{ES} value. Because of this, whenever R_{ES} is referred to in this article, it deals with a device not the material.

2.3.1. Evaluation of R_{ES}

The most widely accepted method to evaluate R_{ES} is through the analysis of the *IR* drop or voltage variation at the initial stage of the discharging curve from CCCD tests. By applying Ohm's law to the *IR* drop, R_{ES} can be acquired readily:

$$R_{ES} = \frac{\Delta V}{\Delta I} \tag{20}$$

where ΔV and ΔI are the voltage and current of the *IR* drop, respectively. A larger charge/discharge current used in the test will usually give rise to a smaller R_{ES}.[61]

Another less common approach is based on the voltage recovery behavior after a current interruption during a discharge process.[108,109] This method is fundamentally the same as the *IR* drop method and yields matching results, and is hence not described in detail here.

Typically, the R_{ES} from EIS test is evaluated using the real part of the complex impedance at 1 kHz and is normally noted in Nyquist plot. Another method, via linear interpolation of the low-frequency part of Nyquist plot to Im(*Z*) = 0, is also used sometimes in literature. An example is provided in **Figure 9** to illustrate these two methods in EIS test, testing a typical commercial SC, 2.7 V/1 F Maxwell cell. Compared to the R_{ES} derived from CCCD test, the value from EIS testing is usually smaller.

2.3.2. Major Affecting Factors

There are two major factors that affect the accuracy of R_{ES} from CCCD test: the dwelling time and the size of SC. CCCD test is usually carried out without dwelling at the peak potential, that is, the discharging starts once the peak potential is reached. However, the practice of non-zero dwelling time is widely adopted in tests, which can greatly influence the final value of R_{ES}. A couple of different dwelling times have been reported: 1 min in the procedure developed by Burke,[110] 5 min in Illinois capacitors,[111] 10 min by Ioxus,[112] etc. Another often overlooked affecting factor on R_{ES} is the size of SCs in terms of cell capacitance as defined in **Table 2**. The two factors are discussed in detail below.

To the best of our knowledge, there has been no study carried out to examine the influence of dwelling time on R_{ES}. Therefore, by using the same 2.7V/1F SC from Maxwell Technologies, we acquired and presented its CCCD plots with different dwelling time varying from 0–30 min in **Figure 10**a. Figure 10b demonstrated the impact of dwelling time on the resulting R_{ES}. To clearly display the variation of CCCD plots, we selected and enlarged the upper region of the plots with dwelling time of 0 min and 1 min, and they are shown separately in Figure 10c,d, with the potential and current changes marked in black and blue, respectively. If *I* is the constant current applied, then in the case of 0 min dwelling time, the current change is:

$$\Delta I \cong 2I \tag{21}$$

Whereas in the cases of >0 min dwelling time,

$$\Delta I \cong I \tag{22}$$

Combined with the potential change, as shown in Figure 10b: we have at 0 min dwelling time, a much smaller R_{ES} ≈ 0.93 ohms, compared to 1.47 ohms from dwelling time >0 min cases.

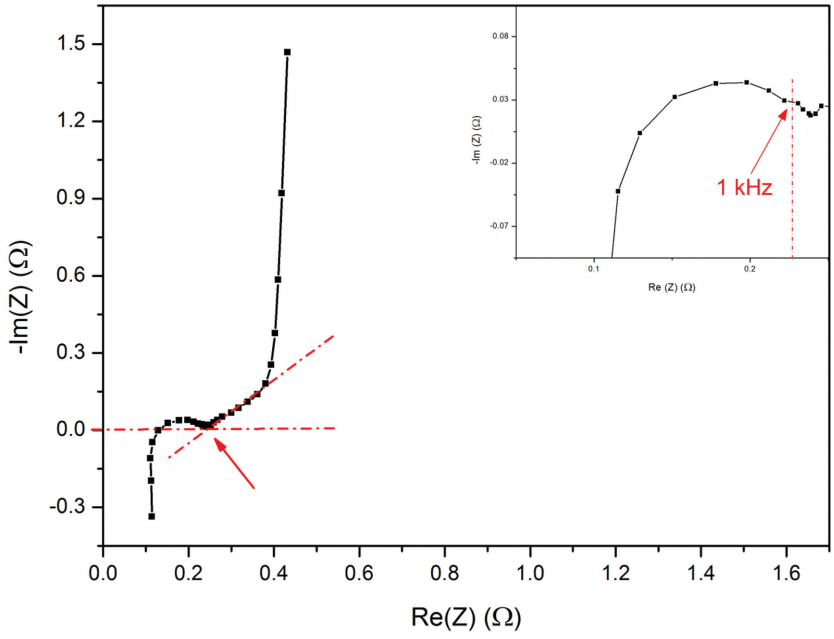

Figure 9. The Nyquist plot of 2.7 V/1 F Maxwell SC with R_{ES} determination methods marked in red.

Table 2. Defined SC size based on total cell capacitance.

	Micro cell	Small cell	Medium cell	Large cell	Ultra-large cell
C_T	<1 mF	1 mF – 10 F	10 F – 100 F	100 F – 1000 F	>1000 F

It is still not clearly understood how the cell size affects the CCCD results. It is, however, generally accepted that the *IR* drop method works fine only for small SCs, and a steady-state voltage drop method should be used for large SCs. As shown in **Figure 11**a, the steady-state voltage drop ΔV_2, rather than the *IR* drop ΔV_1, is obtained through the back extrapolation of the potential trace; it is larger than ΔV_1 by almost 50%, thus leading to a nearly 50% increase in R_{ES}. An actual example is provide in Figure 11b reported by Burke et al.[61] Studies[61,88] have been conducted and the results demonstrated that more accurate power performance can be estimated using ΔV_2 for large cells, and it is therefore recommended.

2.4. Operating Voltage V_o

Strictly speaking, the operating voltage V_o refers to the potential applied to the system or the suitable potential window within which a cell normally operates. In this article, the term is sometimes interchangeable with cell voltage or rated potential, which represents the maximum voltage a cell can endure.

2.4.1. *Evaluation of V_o*

Both CV and CCCD tests can be used to determine V_o of either the SC materials or the devices. However actual testing of this maximum potential carries the risk of destroying the cell. An expedient method is usually applied, with an example given in **Figure 12** using an asymmetric MnO_2/AC capacitor,[81] where V_o can be achieved by starting with a lower voltage applied to the cell, and then slowly increasing the voltage until a spike appears at the boundary of the potential window as seen in the figure.

2.4.2. *Major Factors Affecting V_o*

Two major factors affecting V_o for SC devices include the solvent in electrolytes and the cell configuration. In aqueous systems, a cell can usually be charged to 1.0 V, limited by the

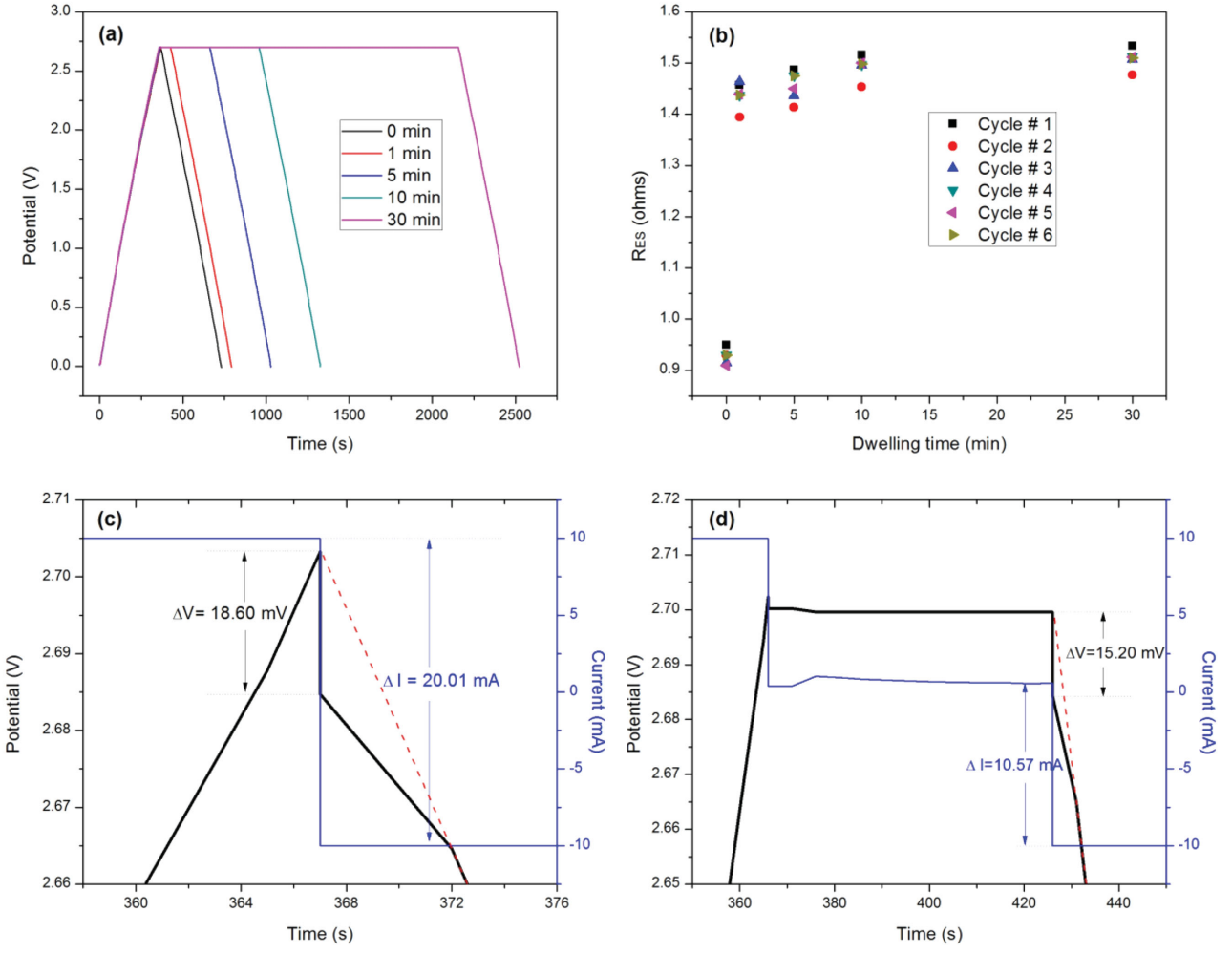

Figure 10. CCCD result of 2.7 V/1 F Maxwell SC tested at different dwelling time from 0 to 30 min: a) overall CCCD plots of one cycle; b) averaged R_{ES} values from first six cycles; enlarged upper region of the CCCD plots at dwelling time of c) 0 min and d) 1 min.

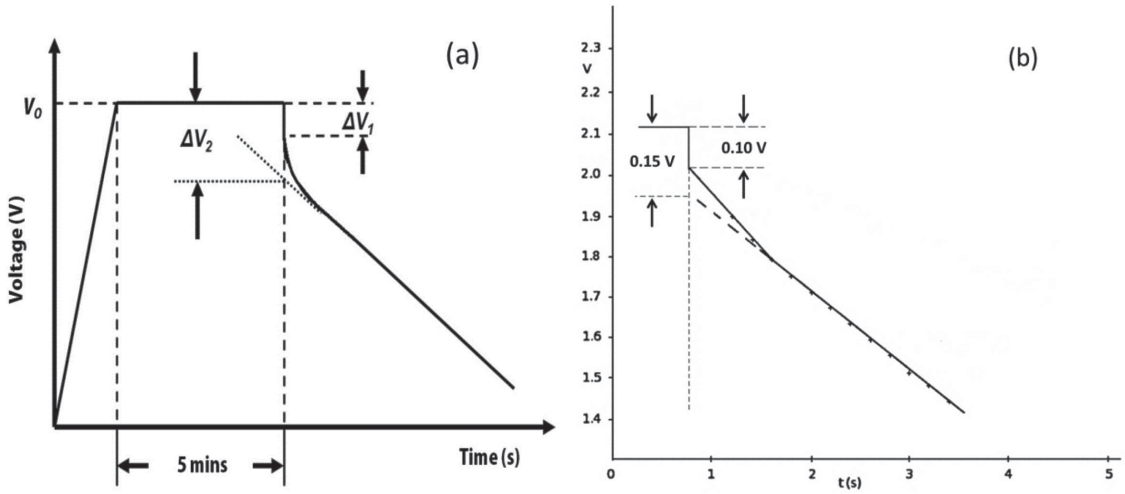

Figure 11. a) A typical CCCD plot for large SCs with *IR* drop and steady-state voltage drop marked as ΔV_1 and ΔV_2, and b) a real case illustration of the discharge part via Skeleton Tech 1600F SC. Reproduced with permission.[61] Copyright 2010, Elsevier.

thermodynamic decomposition potential of water at room temperature. V_o in organic solvent electrolyte varies between 2.3 and 2.7 V.[23,113–117] As both energy and power densities are proportional to V_o^2 much effort has been dedicated to developing novel electrolytes that can endure high voltage (>3 V). Room-temperature ionic liquids (RTILs) are considered to be the most promising candidate by which high V_o values between 3.0 and 6.0 V can be achieved in research labs.[118,119] In addition, various mixtures of different RTILs, or RTIL and organic solvents, also appear to be attractive.[120,121]

The other factor influencing V_o is the cell configuration. In an asymmetric system, V_o can be increased by using different SC materials so as to introduce additional electrochemical potential difference.[81] This way, even in aqueous systems, V_o can reach 2.0–2.3 V,[35,81,122,123] giving rise to much improved energy storage.[35,124]

In conclusion, for SC materials, all three techniques, i.e., CV, EIS and CCCD tests, can be employed with different emphases. However, for SC devices, the most effective and accurate approach is CCCD testing to measure the cell capacitance, equivalent series resistance, and operating voltage.[61] Subsequently, the time constant, energy and power densities, and leakage and maximum current of SC devices can be derived from these three core parameters.

2.5. Time Constants

The time constant τ is only for SC devices and defined as the product of R_{ES} and C_T as shown in Equation (23) using the equivalent RC circuit for a SC in Figure 8. A smaller τ reflects a better responsiveness of the device, and for most of commercial SCs, τ normally ranges from 0.5 to 3.6 s.[125]

$$\tau = R_{ES}C_T \tag{23}$$

Based on the RC circuit model, the voltage of SC device changes by 36.8% at time $t = \tau$, and by 98% at time $t = 4\tau$, during the charge/discharge processes.

Normally τ is fixed around a certain value for SCs produced using the same technology, for example 0.55 s from Maxwell Technologies, 1.1 s from NessCap and 3.8 s from JSR Micro, as reported by Burke.[125] Consequently, C_T and R_{ES} for the same type of SCs are inversely proportional to each other when τ is fixed. An example is shown in **Table 3** for BCAP SCs from Maxwell Technologies, and we calculated the corresponding τ values.

Attention has to be paid here not to confuse this τ with another "relaxation time constant", τ_0, as occurred in ref. [86,126,127] τ_0 was proposed by Simon et al. based on EIS tests.[64] Using the same 2.7 V/1 F Maxwell SC and plotting both

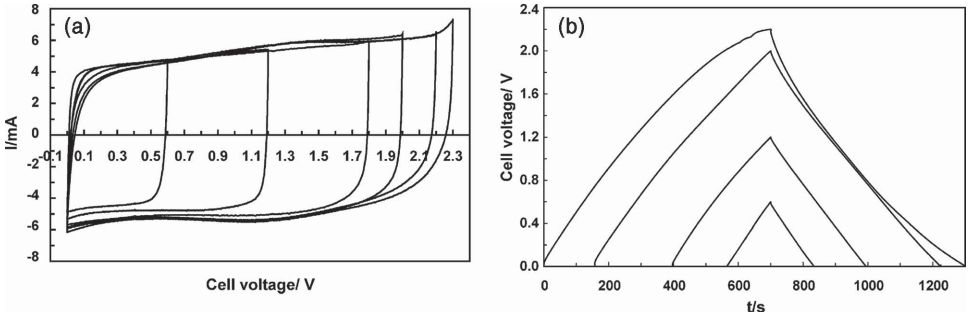

Figure 12. An illustration of V_o determination methods using a) CV and b) CCCD tests. Reproduced with permission.[81] Copyright 2006, Elsevier.

Table 3. C_T and R_{ES} for BCAP SCs from Maxwell Technologies.

C_T [F]	1	3.3	5	10	25	50	100	310	350	650	1200	1500	2000	3000
R_{ES} [mΩ]	700	290	170	75	42	20	15	2.2	3.2	0.8	0.58	0.47	0.35	0.29
τ [s]	0.7	0.96	0.85	0.75	1.05	1.0	1.5	0.68	1.12	0.52	0.7	0.71	0.7	0.87

Re(*C*) and Im(*C*) vs. frequency, as shown in **Figure 13**, τ_0 is marked at the position where the imaginary part of the capacitance reaches its maximum at frequency f_0, and can be calculated to be 3.86 s using Equation (24):

$$\tau_0 = 1/f_0 \tag{24}$$

It is much larger than τ = (1.34 F)(1.44 Ω) = 1.94 s. In fact, such difference was revealed in the same paper by Simon et al.[64] They reported τ = 0.7 s, but τ_0 = 10 s for their symmetric AC-based SC with mass loading of 15 mg cm^{-2}.

2.6. Power and Energy Densities

Of the performance metrics for all kinds of energy storage and conversion systems, power density and energy density are the most directly relevant to the end applications and hence are the parameters used most often for performance evaluation.

They normally are evaluated gravimetrically or volumetrically in W kg^{-1} or W L^{-1} for power density to describe the efficacy in energy uptake/delivery; and in Wh kg^{-1} or Wh L^{-1} for energy density to demonstrate the amount of electrical energy stored or deliverable. For effective comparison with other EES devices, a Ragone plot[128] is shown in **Figure 14**. The diagonal time line is a representative line for the so-called "characteristic time",[129] a reflection of running time of the devices at the rated power. The actual running times of EES devices vary a lot, depending on the load or discharging rate; the so-called rate dependence as discussed in 3.3 below.

2.6.1. Power Density

The outstanding power performance of SC devices is one of their major merits. The most widely used calculation method for the maximum power density is shown as:

$$P_D = \frac{V_o^2}{4R_{ES}\Pi} \tag{25}$$

This maximum power delivery can only be realized when the load has the identical resistance as R_{ES}, often referred to as the matched load condition.

Of course in practice, the load resistor often does not match R_{ES}. As necessary supplements, there are several other methods proposed to compute the actual power capacity. Three most widely adopted methods are DOE-FreedomCar,[134] IEC 62576[135] and the pulse energy efficiency (PEE)[125] methods, and one can refer to ref. [79,134,136] for detailed discussions. **Table 4** provides the resulting actual power densities with respect to the maximum P_D based on the different test procedures and the data published by Burke.[79,137] Therefore, although the maximum value P_D is widely used for comparison, one has to keep in mind that it does not usually represent the actual deliverable power density, and one must choose the proper percentage below based on the corresponding applications.

In principle, a further boosted P_D value is always beneficial, but little effort[138] has been devoted to this because SCs already have relatively high P_D.

2.6.2. Energy Density

The electricity stored in or released from SCs can be evaluated through the integration of the working diagrams as illustrated in **Figure 15** for EDLCs or PCs, and **Figure 16** for HCs, where the difference in shape is caused again by their distinct charge storage mechanisms. In either case, the stored electric energy can be obtained from the charging curve, and the deliverable energy from the discharging curve. The ratio of the two is called the energy efficiency of the cell, an indicator of the difference between the two parts of the curve. Calculations for the stored electricity are illustrated below.

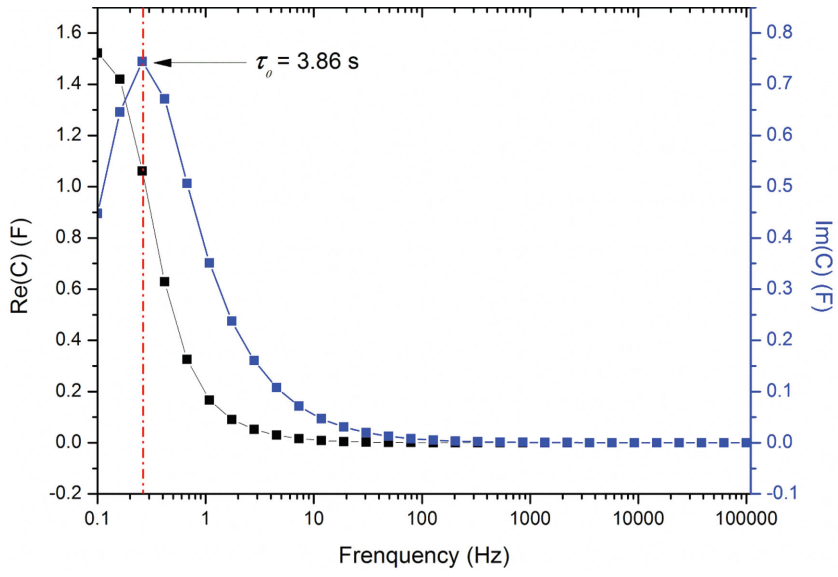

Figure 13. Dependence of real and imaginary capacitances over frequency for 2.7 V/1 F Maxwell SC with the relaxation time constant τ_o indicated.

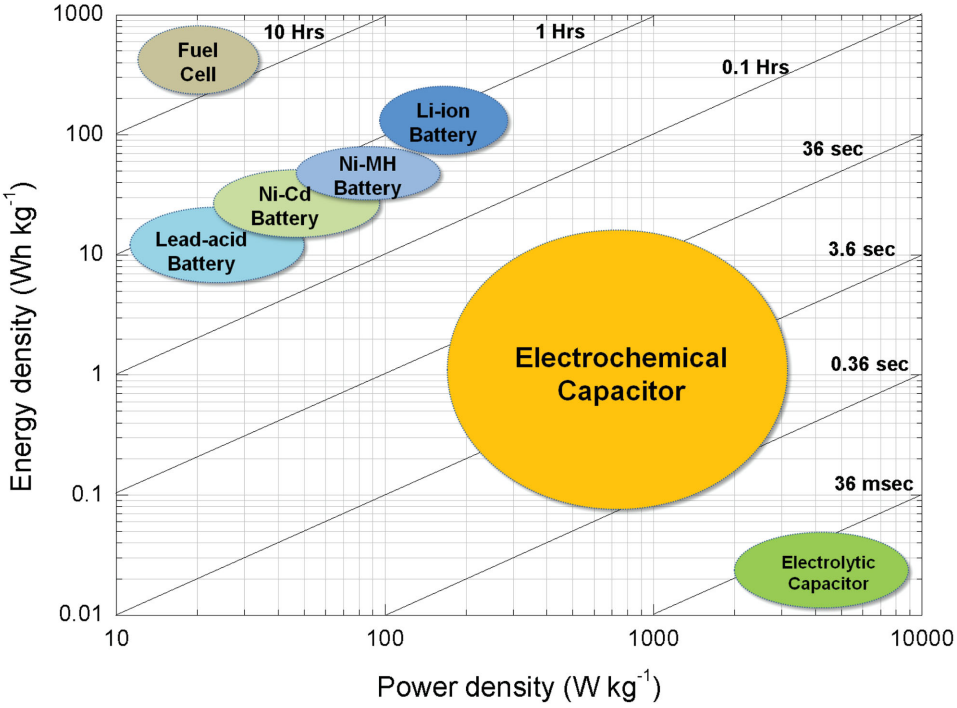

Figure 14. An illustration of the power and energy densities for several EES devices via Ragone plot. The plot is based on data from ref. [125,130–133]

a. For EDLCs and PCs with linear charge/discharge curves, the integration of the working diagram turns into the calculation of triangle area as shown in Figure 15, therefore:

$$E_D = \int_0^Q V_o \, dq = \frac{1}{2} V_o Q \tag{26}$$

Substituting Equation (2) into Equation (26) yields,

$$E_D = \frac{1}{2\Pi} C_T V_o^2 \tag{27}$$

Dividing by 3600 converts E_D in Joule Π^{-1} to watt hour Π^{-1}:

$$E_D = \frac{\frac{1}{2} C_T V_o^2}{3600\Pi} \tag{28}$$

It is worth mentioning that by combining Equation (23), (25) and (27), the relationship between P_D and E_D for EDLCs is given below:

$$\frac{E_D}{P_D} = 2R_{ES}C_T = 2\tau \tag{29}$$

Table 4. Power densities obtained from different methods.

	Matched load	USABC	IEC	PPE
Power density	$P_D = V_o^2/(4\Pi R_{ES})$	50% P_D	48% P_D	11.25% P_D

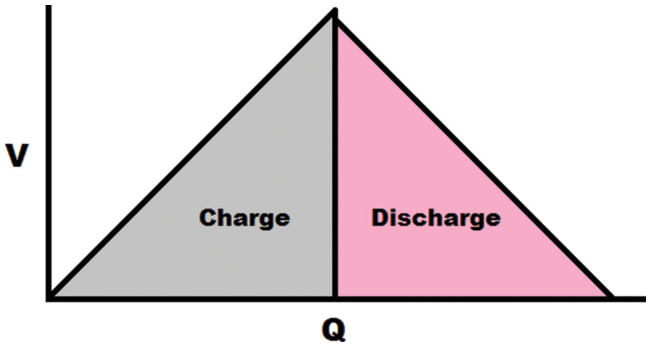

Figure 15. Representative working diagram from CCCD test for EDLCs and PCs.

This equation indicates that the energy and maximum power densities are closely coupled by the cell time constant $\tau = R_{ES}C_T$. Although E_D can be increased in Equation (27) by improving either the capacitance or operating voltage, raising the capacitance alone will simultaneously increase the time constant τ,

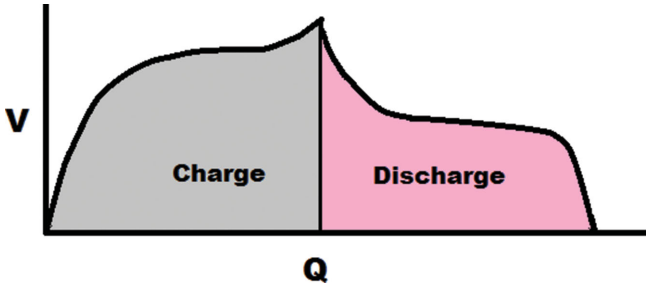

Figure 16. Representative working diagram from CCCD test for HCs.

leading to a less responsive cell, assuming R_{ES} unchanged. Boosting the voltage can considerably enlarge both P_D and E_D, while still maintaining the same τ value. Although increasing E_D is the major stride for SC community, extra attention is required at the same time for the possible associated changes in τ or P_D.

However, for HCs with nonlinear charge/discharge curves as shown in Figure 16, the integration of the diagram has no simple solution, depending on the specific shape of the curve, so that:

$$E_D = \int_0^Q V\,dq = \int_0^{t_Q} VI\,dt \tag{30}$$

Dividing by 3600 and Π, one can still obtain the energy density in watt hour Π^{-1}:

$$E_D = \int_0^Q V\,dq = \frac{\int_0^{t_Q} VI\,dt}{3600\Pi} \tag{31}$$

That is, Equation (28) is not valid for HCs with nonlinear charge/discharge curves, and for them Equation (31) has to be used.

2.7. Leakage and Maximum Peak Currents

For SC devices, an additional yet useful parameter is the leakage current, widely used in industry to evaluate the capability of SCs to maintain the rated potential when not in use. Normally, it is recorded as the compensating current that applied to hold a fully charged SC after 72 h.

Another similar device parameter is the maximum peak current, which usually appears in the specifications for commercial SCs. It is evaluated by discharging a fully charged SC device from V_0 to ½ V_0 in 1 s, and calculated as:

$$I_{max@1s} = \frac{\frac{1}{2}C_T V_0}{C_T R_{ES} + 1} \tag{32}$$

2.8. Cycle Life and Capacitance Retention Rate

Long cycle life of SC devices is one of their major merits and leads to the so-called "fit-and-forget" benefits, which are highly desirable for certain applications. But this extremely long cycle life (>1 000 000 cycles) also makes it difficult to directly measure it. Another term, the capacitance retention rate is therefore used to indirectly estimate the cycle life of SCs. It is easily obtained in CCCD test by comparing the capacitance after given thousands of cycles with that of the first cycle. One attempt[139] was made recently by continuously test SCs for 3.8 years, and the results showed that the capacitance retention rate is decreasing almost linearly with the square root of the number of cycles. Further validations are needed to establish this relationship, but it does give us a glimpse on the time demanding nature of the direct measurement of cycle life.

3. Inconsistencies in Evaluation of SCs

3.1. Causes for the Inconsistencies

For any comparison to be meaningful, the same or consistent metrics and test methods must be used. As demonstrated and discussed in this article so far, it is easy to see why performance evaluation of SCs has become so prevalently plagued by inconsistencies, and where such inconsistencies are originated. Herein, the common causes are listed below: a) different instruments or calculation method used, i.e., CV, CCCD or EIS; b) different experiment setups: three-electrode, and symmetric and asymmetric two-electrode configurations; c) Differences in electrode fabrication: Mass loading, electrode thickness and density; d) different base Π used: volume or mass; active material only, or combined with additives, binders; single or two electrodes; with or without electrolyte, or the whole cell; e) different test conditions applied (rate dependency): scan rate in CV, charge/discharge current in A g^{-1}, mA cm^{-2}, or mA F^{-1} for CCCD tests.

The inconsistencies caused by a, b, and c in the list have been discussed in the preceding sections. The effects of improper use of the base Π and with the rate dependency are examined below.

3.2. Device Performance vs. Material Property

Although this issue has been dealt with above, the difference between device performance and material property can be huge, often overlooked, and may play a critical role in performance evaluation for any EES system. A recent paper by Gallagher et al.[140] emphasizes such difference in the case of lithium-air batteries. To substantiate the discussion, some useful information from several SC manufacturers, including Maxwell Technologies, WIMA, Nesscap, and Ioxus,[113–116] is collected and analyzed here. Because of the fact that the mainstream SC material in industry is still activated carbon (AC), only AC-based SCs are considered.

For SC devices, their energy and power densities are summarized as: E_D ranging from 1 to 6 Wh kg^{-1} or 2 – 8 Wh L^{-1}; and P_D ranging from 2 to 20 kW kg^{-1} or 4 to 30 kW L^{-1}. The same devices but for SC materials (AC), with C_S of 100 F g^{-1} and 70 F cm^{-3}[70] the parameters are summarized as: E_D ranging from 15 to 25 Wh kg^{-1} or 12 to 18 Wh L^{-1}; and P_D ranging from 20 to 120 kW kg^{-1} or 13 to 80 kW L^{-1}.

The substantial difference between device performance and material properties is clearly demonstrated above. This is due to the fact that only a small portion of the weight and volume of SC devices are composed of electrode materials, around 2.5–30 wt% and 10–50 vol%, and this may even smaller for micro-SCs.[95,105,106] Similar relationships between the weight and volume ratios of electrode material over the whole cell and cell capacitance are observed as illustrated in **Figure 17** based on Maxwell BCAP SCs.[141] What is worrisome is that in most of the published scientific literature,[63,68,78,90,96,142–150] no distinction has been made explicitly between the device performance and material properties, leaving room for potential misinformation and confusion.

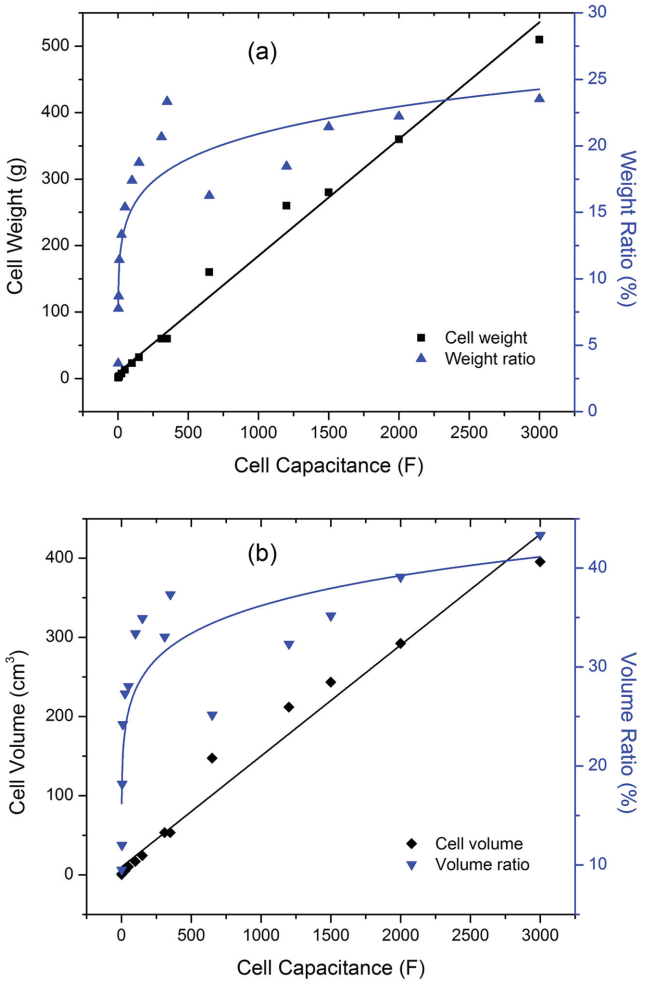

Figure 17. a) Cell weight and weight ratio and b) cell volume and volume ratio between the electrode material and the whole cell, as functions of cell capacitance. Data from Maxwell BCAP SCs.[141]

Admittedly, it may often be impracticable to request energy and/or power densities for the whole device in a publication, for in frequent cases where the focus is to probe for novel materials, the final products may not be in the form of a well packaged cell. Also in searching for new cell design and more advanced manufacturing processes,[38,47,57,86] different research groups are likely using rather distinct types of current collectors, separators, packaging materials, and packaging methods[45,68,73,85] to report all such details for a whole cell in all the publications may not be highly feasible. It is therefore much more convenient to report and compare the electrodes used. Based on the specific requirement of targeted application, either gravimetric or volumetric value or both should be reported. Also, similar to the determination of C_S, the mass or volume of one entire electrode including the conductive additive and polymer adhesive is recommended to be used in the calculation for macro-SCs ($C_T > 1$ mF). In addition, the mass loading (mass/area) or packing density (mass/volume) and thickness of the electrode are strongly suggested to be reported explicitly for fair comparison.

For micro-SCs ($C_T < 1$ mF) where mass and volume are too small, and the footprint area (cm^2) of one electrode is used instead; their energy and power densities (also capacitance) must be normalized by this footprint area. The footprint area of one electrode is recommended to be used in calculations. As a necessary supplement in such particular cells, the thickness of the electrode, the current collector, electrolyte, and even the substrate must be clearly indicated as well.

3.3. Rate Dependence

The rate dependence of all EES devices is a universal, yet thorny issue.[151] For example, batteries are usually affixed with a rated energy C_o in Ampere hour at a rated potential. However, in actual use, how much energy this battery can actually deliver to a load depends on the discharge/recharge rate.[151] In other words, if a load drains this battery in a shorter time period, the actual energy supplied will be $C_A < C_o$. Peukert's law[151,152] is usually applied to describe this phenomena as:

$$C_A = it = \frac{C_o}{(t_o/t)^{k-1/k}} \tag{33}$$

And therefore the current,

$$i = \frac{C_o (t_o/t)^{k-1}}{t_o} \tag{34}$$

Where t_o is the discharge rate or time (hrs) used to measure C_o, k is the Peukert's factor, usually $1.1 < k < 1.6$ for batteries. This k value indicates the degree of dependency of C_A on discharge rate, and a smaller value is more desirable, implying less rate independency.[151]

To address this issue, the C-rate scheme has been proposed and widely used to scale the charge and discharge current for batteries. Different batteries are rated differently, i.e., with different k values, based on the kinetics of the battery chemistry involved. If a battery is rated at nC, the discharging time will be fixed at around $1/n$ hours,[153] i.e., if rated at 2C, for example, batteries will be completely discharged in 0.5 h. By fixing the discharge or recharge time, this C-rate system tackles successfully the issue of rate dependency for batteries with little confusion. **Figure 18** is constructed using both Equation (33) and (34) to illustrate the actual energy deliverable C_A and the electric current i, as functions of both discharge time and the C-rate level, where one can easily locate the C_A and i for a given pair of discharge time and C-rate level.

For SCs, similar rate dependence has been long and widely recognized,[55,57,59,73,78,125,154–157] yet poorly analyzed and understood. Also similar to the C-rate system for batteries, a 60 s discharge/recharge time is recommended for SCs.[32] This 60 s discharge/recharge time or 60C discharge rate can settle the inconsistencies caused by the different test conditions in CCCD tests, i.e., A g^{-1}, mA cm^{-2}, mA cm^{-3}, or mA F^{-1},[142,144,158,159] and can be used as a guide to determine the proper scan rate used in CV tests: $v = 1/60$ V s^{-1} (≈16.7 mV s^{-1}) for 1 V systems; $v = 2.3/60$ V s^{-1} (≈38.3 mV s^{-1}) for 2.3 V ones; and $v = 2.7/60$ V s^{-1} (45 mV s^{-1}) for 2.7 V ones.

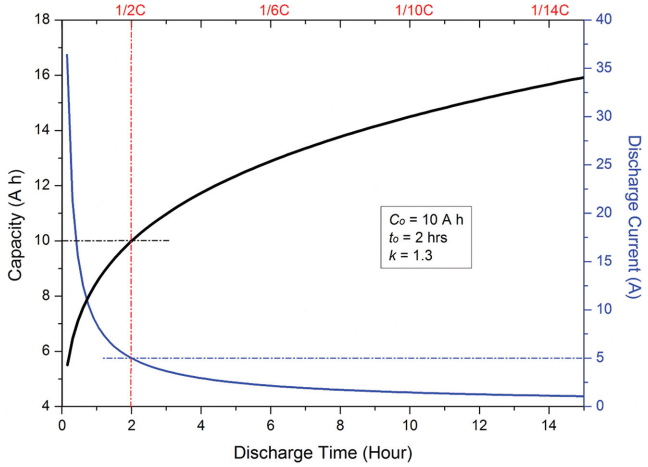

Figure 18. An illustration of Peukert's curve for batteries with the use of ½C marked by dashed lines.

To demonstrate the rate dependency and the use of 60 s discharge/recharge time for SCs, we collected the test data of a 1450F EDLC[13] and a 2000F hybrid SC[61] and fitted them nicely using again both Equation (33) and (34) as shown in **Figure 19**. Consequently, Peukert's factor $k \approx 1.02$ is estimated for the EDLC and $k \approx 1.06$ for hybrid SC, reflecting the different kinetics of charge storage/release mechanism in each system.

4. Summary and Recommendations

We have identified and examined the inconsistencies that exist in the current practices for the evaluation of supercapacitors. Such inconsistencies are caused by some common sources including different test instruments, evaluation methods, and other related factors. In summary, a fair comparison is only possible if we: 1) employ the same instruments under consistent test conditions and experimental setups; 2) derive the performance metrics using consistent calculation methods; and 3) compare the comparables.

Moreover, a few more specific recommendations are proposed as follows: 1) Apply 60 s discharge or recharge time to address the rate dependency of supercapacitors so as to produce comparable parameters. 2) Use CCCD tests to determine all the three core parameters, i.e., the capacitance, equivalent series resistance, and operating voltage, and subsequently the time constant, energy and power densities, and leakage/maximum peak current for supercapacitor devices. 3) Use CV or CCCD tests on a three-electrode setup to examine the operating voltage and specific capacitance of supercapacitor materials. 4) Use EIS to study the transient impedance behavior and frequency response of supercapacitor materials and devices. 5) Differentiate between the device performance and material properties, and clearly state the mass loading, thickness, density of the electrode. 6) Keep in mind the interconnections between the energy density, maximum power density and the cell time constant: they cannot be altered individually. It should also be noted that increasing the operating voltage by using advanced electrolyte or novel cell design is the most effective way to raise both energy and power densities, while still upholding the τ value.

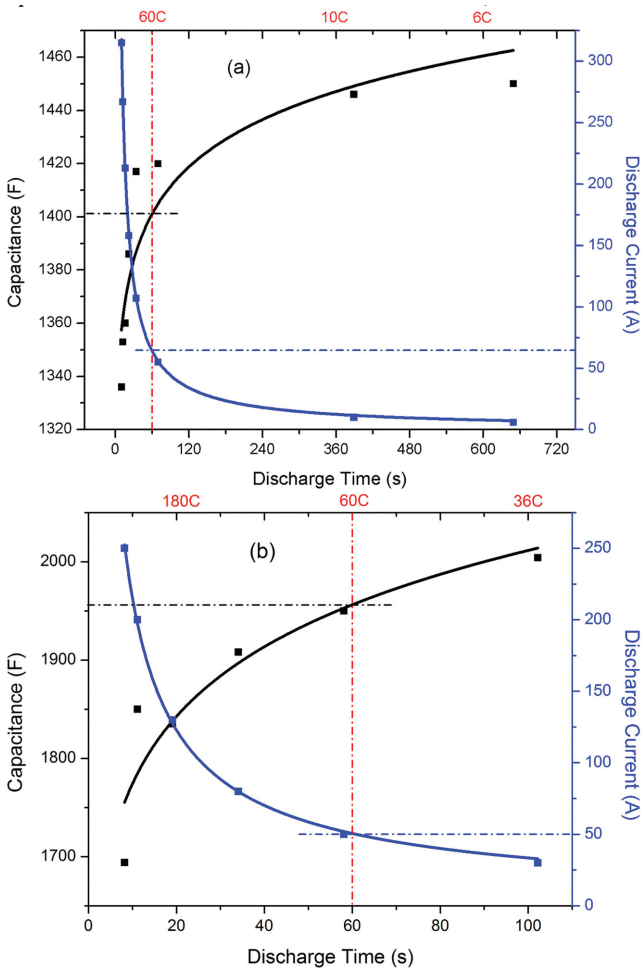

Figure 19. An illustration of Peukert's curves for a) a 1450F EDLC and for b) a 2000F hybrid capacitor with the use of 60C marked by dashed lines.

It is fitting to end this article by quoting from the paper by Simon et al.[32] "The prospect of developing materials with the energy density of batteries and the power density and cycle life of supercapacitors is an exciting direction that has yet to be realized. Whether to approach these goals by increasing the power density of battery materials or increasing the energy density of supercapacitors is one of the enticing features of the field. However, there needs to be clarity in the terminology used in combination with appropriate measurements and analyses. Proper evaluation of new materials and their charge storage mechanisms will facilitate progress in this important field of electrical energy storage."

Acknowledgements

This work was supported by California Energy Commission EISG Project 57470A/12–02TE, as well as by NIFA projects CA-D*-TXC-6426-RR and CA-D*-TXC-7694-H.

Received: August 12, 2014
Revised: September 24, 2014
Published online: December 12, 2014

[1] R. B. Erb, *Acta Astronaut.* **1997**, *40*, 345.
[2] X. C. Wei, E. P. Li, Y. L. Guan, Y. H. Chong, *J. Electromag. Wave* **2009**, *23*, 925.
[3] M. R. Patel, *Wind and Solar Power Systems: Design, Analysis, and Operation*, CRC Press, Boca Raton, FL, USA **2012**.
[4] D. Rastler, *Electric Energy Storage Technology Options: A White Paper Primer on Applications, Costs, and Benefits*, EPRI, Palo Alto, CA, USA **2010**.
[5] W. Martin, J. B. Ralph, *Chem. Rev.* **2004**, *104*, 4245.
[6] L. Dingrando, N. Hainen, C. Wistrom, K. Tallman, *Glencoe Chemistry: Matter and Change*, Glencoe/Macmillan/McGraw-Hill, New York **2007**, Ch. 21.
[7] P. Kurzweil, M. Chwistek, R. Gallay, presented at the 2nd European Symposium on Super Capacitors & Applications (ESSCAP), Lausanne, CH, 2–3 November **2006**.
[8] H. Omanda, T. Brousse, C. Marhic, D. M. Schleich, *J. Electrochem. Soc.* **2004**, *151*, A922.
[9] J. M. Tarascon, M. Armand, *Nature* **2001**, *414*, 359.
[10] C. Daniel, J. O. Besenhard, *Handbook of Battery Materials*, Wiley-VCH, Weinheim, Germany **2011**, Ch. 27.
[11] A. F. Burke, presented at MRS Spring Meeting, San Francisco, CA, 24–28 March **2008**.
[12] C. Arbizzani, M. Mastragostino, F. Soavi, *J. Power Sources* **2001**, *100*, 164.
[13] M. Arulepp, J. Leis, M. Lätt, F. Miller, K. Rumma, E. Lust, A. F. Burke, *J. Power Sources* **2006**, *162*, 1460.
[14] L. L. Zhang, X. S. Zhao, *Chem. Soc. Rev.* **2009**, *38*, 2520.
[15] M. A. Guerrero, E. Romero, F. Barrero, M. I. Milanes, E. Gonzalez, *Prz. Elektrotech.* **2009**, *85*, 188.
[16] C. S. Du, N. Pan, *J. Power Sources* **2006**, *160*, 1487.
[17] X. Zhao, B. M. Sánchez, P. J. Dobson, P. S. Grant, *Nanoscale* **2011**, *3*, 839.
[18] B. E. Conway, *J. Electrochem. Soc.* **1991**, *138*, 1539.
[19] C. Arbizzani, M. Mastragostino, L. Meneghello, *Electrochim. Acta* **1995**, *40*, 2223.
[20] C. Arbizzani, M. Mastragostino, L. Meneghello, *Electrochim. Acta* **1996**, *41*, 21.
[21] M. Mastragostino, R. Paraventi, A. Zanelli, *J. Electrochem. Soc.* **2000**, *147*, 3167.
[22] B. Dyatkin, V. Presser, M. Heon, M. R. Lukatskaya, M. Beidaghi, Y. Gogotsi, *ChemSusChem* **2013**, *6*, 2269.
[23] P. Kurzweil, M. Chwistek, *J. Power Sources* **2008**, *176*, 555.
[24] SNE Research, Ultra Capacitor – Recent Technology and Market Forecast (2020), October **2012**.
[25] B. E. Conway, *Electrochemical Supercapacitor: Scientific Fundamentals and Technological Applications*, Kluwer Academic/Plenum Publishers, New York **1999**.
[26] H. Wang, L. Pilon, *J. Phys. Chem. C* **2011**, *115*, 16711.
[27] H. von Helmholtz, *Ann. Phys.* **1853**, *165*, 211.
[28] H. von Helmhotz, *Pogg. Ann.* **1853**, *LXXXIX*, 211.
[29] A. J. Bard, L. R. Faulkner, *Electrochemical Methods: Fundamentals and Applications*, Wiley, New York **2000**.
[30] H. I. Becker, (General Electric) *U.S.Patent 2800616*, **1957.**
[31] B. E. Conway, V. Birss, J. Wojtowicz, *J. Power Sources* **1997**, *66*, 1.
[32] P. Simon, Y. Gogotsi, B. Dunn, *Science* **2014**, *343*, 1210.
[33] S. Trasatti, G. Buzzanca, *J. Electroanal. Chem. Interfacial Electrochem.* **1971**, *29*, App. 1.
[34] T.-C. Liu, W. G. Pell, B. E. Conway, *J. Electrochim. Acta* **1997**, *42*, 3541.
[35] B. E. Conway, *J. Electrochem. Soc.* **1991**, *138*, 1539.
[36] T.-C. Liu, W. G. Pell, B. E. Conway, S. L. Roberson, *J. Electrochem. Soc.* **1998**, *145*, 1882.
[37] J. W. Long, D. Bélanger, T. Brousse, W. Sugimoto, M. B. Sassin, O. Crosnier, *MRS Bull.* **2011**, *36*, 513.
[38] M. Toupin, T. Brousse, D. Bélanger, *Chem. Mater.* **2004**, *16*, 3184.
[39] K. Naoi, P. Simon, *Electrochem. Soc. Interface* **2008**, *17*, 34.
[40] J. P. Zheng, *J. Electrochem. Soc.* **2003**, *150*, A484.
[41] A. L. Beliakov, A. M. Brintsev, presented at the 7th International Seminar on Double-layer Capacitors and Similar Energy Storage Devices, Deerfield Beach, FL, 8–10 December **1997**.
[42] K. Naoi, W. Naoi, S. Aoyagi, J.-i. Miyamoto, T. Kamino, *Acc. Chem. Res.* **2012**, *46*, 1075.
[43] A. S. Arico, P. Bruce, B. Scrosati, J.-M. Tarascon, W. V. Schalkwijk, *Nat. Mater.* **2005**, *4*, 366.
[44] K. Naoi, S. Ishimoto, J.-i. Miyamoto, W. Naoi, *Energy Environ. Sci.* **2012**, *5*, 9363.
[45] W. J. Cao, J. P. Zheng, *J. Power Sources* **2013**, *213*, 180.
[46] M. D. Stoller, S. Murali, N. Quarles, Y. Zhu, J. R. Potts, X. Zhu, H. W. Ha, R. S. Ruoff, *Phys. Chem. Chem. Phys.* **2012**, *14*, 3388.
[47] M. R. Lukatskaya, O. Mashtalir, C. E. Ren, Y. Dall'agnese, P. Rozier, P. L. Taberna, M. Naguib, P. Simon, M. W. Barsoum, Y. Gogotsi, *Science* **2013**, *341*, 1502.
[48] I. N. Varakin, A. D. Klementov, S. V. Litvinenko, N. F. Starodubtsev, A. B. Stepanov, presented at the 8th International Seminar on Double-layer Capacitors and Similar Devices, Deerfield Beach, FL, 7–9 December **1998**.
[49] J. Furukawa, T. Takada, D. Monma, L. T. Lam, *J. Power Sources* **2010**, *195*, 1241.
[50] A. Cooper, J. Furakawa, L. Lam, M. Kellaway, *J. Power Sources* **2009**, *188*, 642.
[51] L. T. Lam, R. Louey, N. P. Haigh, O. V. Lim, D. G. Vella, C. G. Phyland, L. H. Vu, J. Furukawa, T. Takada, D. Monma, T. Kano, *J. Power Sources* **2007**, *174*, 16.
[52] L. T. Lam, R. Louey, *J. Power Sources* **2006**, *158*, 1140.
[53] F. Beguin, E. E. Frackowiak, *Supercapacitors: Materials, Systems and Applications*, Wiley-VCH, Weinheim, Germany **2013**.
[54] S. Ardizzone, G. Fregonara, S. Trasatti, *Electrochim. Acta* **1990**, *35*, 263.
[55] J. W. Kim, V. Augustyn, B. Dunn, *Adv. Energy Mater.* **2012**, *2*, 141.
[56] X. Wang, G. Li, Z. Chen, V. Augustyn, X. Ma, G. Wang, B. Dunn, Y. Lu, *Adv. Energy Mater.* **2011**, *1*, 1089.
[57] T. Brezesinski, J. Wang, S. H. Tolbert, B. Dunn, *Nat. Mater.* **2010**, *9*, 146.
[58] K. Brezesinski, J. Wang, J. Haetge, C. Reitz, S. O. Steinmueller, S. H. Tolbert, B. M. Samarsly, B. Dunn, T. Brezesinski, *J. Am. Chem. Soc.* **2010**, *132*, 6982.
[59] J. Wang, J. Polleux, J. Lim, B. Dunn, *J. Phys. Chem. C* **2007**, *111*, 14925.
[60] V. Augustyn, J. Come, M. A. Lowe, J. W. Kim, P.-L. Taberna, S. H. Tolbert, H. D. Abruña, P. Simon, B. Dunn, *Nat. Mater.* **2013**, *12*, 518.
[61] A. Burke, M. Miller, *Electrochim. Acta* **2010**, *55*, 7538.
[62] J. R. Miller, R. A. Outlaw, B. C. Holloway, *Science* **2010**, *329*, 1637.
[63] C. Du, N. Pan, *J. Power Sources* **2006**, *160*, 1487.
[64] P. L. Taberna, P. Simon, J. F. Fauvarque, *J. Electrochem. Soc.* **2003**, *150*, A292.
[65] M. F. Dupont, A. F. Hollenkamp, S. W. Donne, *J. Electrochem. Soc.* **2014**, *161*, A648.
[66] C. Zhao, W. Zheng, X. Wang, H. Zhang, X. Cui, H. Wang, *Sci. Rep.* **2013**, *3*, 2986.
[67] D. Qu, H. Shi, *J. Power Sources* **1998**, *74*, 99.
[68] Y. Zhu, S. Murali, M. D. Stoller, K. J. Ganesh, W. Cai, P. J. Ferreira, A. Pirkle, R. M. Wallace, K. A. Cychosz, M. Thommes, D. Su, E. A. Stach, R. S. Ruoff, *Science* **2011**, *332*, 1537.
[69] X. Yang, C. Cheng, Y. Wang, L. Qiu, D. Li, *Science* **2013**, *341*, 534.
[70] A. Burke, *Electrochim. Acta* **2007**, *53*, 1083.
[71] J. H. Park, O. O. Park, K. H. Shin, C. S. Jin, J. H. Kim, *Electrochem. Solid-State Lett.* **2002**, *5*, H7.

[72] W. Chen, Z. Fan, L. Gu, X. Bao, C. Wang, *Chem. Commun.* **2010**, *46*, 3905.
[73] M. D. Stoller, R. S. Ruoff, *Energy Environ. Sci.* **2010**, *3*, 1294.
[74] M. Stoller, S. Park, Y. Zhu, J. An, R. Ruoff, *Nano Lett.* **2008**, *8*, 3498.
[75] Q. Qu, P. Zhang, B. Wang, Y. Chen, S. Tian, Y. Wu, R. Holze, *J. Phys. Chem. C* **2009**, *113*, 14020.
[76] J. P. Zheng, *Electrochem. Solid-State Lett.* **1999**, *2*, 359.
[77] V. Khomenko, E. Frackowiak, F. Béguin, *Electrochim. Acta* **2005**, *50*, 2499.
[78] S. Zhang, N. Pan, *J. Mater. Chem. A* **2013**, *1*, 7957.
[79] A. Burke, presented at First International Symposium on Enhance Electrochemical Capacitors, Nantes, France, 29 June – 2 July **2009**.
[80] W. Fang, O. Chyan, C. Sun, C. Wu, C. Chen, K. Chen, L. Chen, J. Huang, *Electrochem. Commun.* **2007**, *9*, 239.
[81] V. Khomenko, E. Raymundo-Piñero, F. Béguin, *J. Power Sources* **2006**, *153*, 183.
[82] C. Xu, B. Xu, Y. Gu, Z. Xiong, J. Sun, X. S. Zhao, *Energy Environ. Sci.* **2013**, *6*, 1388.
[83] E. E. Kalu, T. T. Nwoga, V. Srinivasan, J. W. Weidner, *J. Power Sources* **2001**, *92*, 163.
[84] Y. Chen, X. Zhang, P. Yu, Y. Ma, *J. Power Sources* **2010**, *195*, 3031.
[85] S. Zhang, Y. Li, N. Pan, *J. Power Sources* **2012**, *206*, 476.
[86] C. Huang, P. S. Grant, *Sci. Rep.* **2013**, *3*, 2393.
[87] K. H. An, W. S. Kim, Y. S. Park, J.-M. Moon, D. J. Bae, S. C. Lim, Y. H. Lee, *Adv. Funct. Mater.* **2001**, *11*, 387.
[88] W. G. Pell, B. E. Conway, *J. Power Sources* **2004**, *136*, 334.
[89] Z. C. Yang, C. H. Tang, Y. Zhang, H. Gong, X. Li, J. Wang, *Sci. Rep.* **2013**, *3*, 2925.
[90] Z. Tang, C.-h. Tang, H. Gong, *Adv. Funct. Mater.* **2012**, *22*, 1272.
[91] J. Yan, T. Wei, B. Shao, Z. Fan, W. Qian, M. Zhang, F. Wei, *Carbon* **2010**, *48*, 487.
[92] K. S. Ryu, K. M. Kim, N.-G. Park, Y. J. Park, S. H. Chang, *J. Power Sources* **2002**, *103*, 305.
[93] J. R. Miller, presented at the 8th International Seminar on Double Layer Capacitors and Similar Energy Storage Devices, Deerfield Beach, Florida, 7–9 December **1998**.
[94] Y. Gogotsi, P. Simon, *Science* **2011**, *334*, 917.
[95] J. Chmiola, C. Largeot, P. L. Taberna, P. Simon, Y. Gogotsi, *Science* **2010**, *328*, 480.
[96] J. Zhang, X. S. Zhao, *ChemSusChem* **2012**, *5*, 818.
[97] J. Yan, Z. Fan, W. Sun, G. Ning, T. Wei, Q. Zhang, R. Zhang, L. Zhi, F. Wei, *Adv. Funct. Mater.* **2012**, *22*, 2632.
[98] D. Qu, P. Smith, G. Gourdin, T. Jiang, T. Tran, *Chem. Eur. J.* **2012**, *18*, 3141.
[99] H. Jiang, C. Li, T. Sun, J. Ma, *Nanoscale* **2012**, *4*, 807.
[100] G. Yu, L. Hu, M. Vosgueritchian, H. Wang, X. Xie, J. R. McDonough, X. Cui, Y. Cui, Z. Bao, *Nano. Lett.* **2011**, *11*, 2905.
[101] Z. Fan, J. Yan, T. Wei, L. Zhi, G. Ning, T. Li, F. Wei, *Adv. Funct. Mater.* **2011**, *21*, 2366.
[102] J. H. Park, S. Kim, O. O. Park, J. M. Ko, *Appl. Phys. A: Mater. Sci. Process.* **2005**, *82*, 593.
[103] G. Xiong, C. Meng, R. G. Reifenberger, P. P. Irazoqui, T. S. Fisher, *Electroanalysis* **2013**, *26*, 30.
[104] M. Beidaghi, Y. Gogotsi, *Energy Environ. Sci.* **2014**, *7*, 867.
[105] M. F. El-Kady, R. B. Kaner, *Nat. Commun.* **2013**, *4*, 1475.
[106] D. Pech, M. Brunet, H. Durou, P. Huang, V. Machalin, Y. Gogotsi, P. L. Taberna, P. Simon, *Nat. Nanotechnol.* **2010**, *5*, 651.
[107] J. Luo, H. D. Jang, J. Huang, *ACS Nano* **2013**, *7*, 1464.
[108] Maxwell Technologies, Test Procedures for Capacitance, ESR, Leakage Current and Self-Discharge Characterizations of Ultracapacitors, http://www.maxwell.com/products/ultracapacitors/docs/ applicationnote_maxwelltestprocedures.pdf (accessed December 2013).
[109] S. Zhao, F. Wu, L. Yang, L. Gao, A. F. Burke, *Electrochem. Commun.* **2010**, *12*, 242.
[110] P. Simon, A. Burke, *Electrochem. Soc. Interface* **2008**, *17*, 38.
[111] Illinois Capacitors, Supercapacitor technical guide, http://www.illinoiscapacitor.com/pdf/Papers/supercapacitor_ tech_guide.pdf (accessed September 2013).
[112] Ioxus Inc., Representative Test Procedure for Customer Evaluations, http://www.ioxus.com/wp-content/uploads/2013/04/Ioxus-Test-Procedures-for-Customer-Evaluations.pdf (accessed January 2014).
[113] WIMA Spezialvertrieb elektronischer Bauelemente, http://www.wimausa.com/ (accessed September 2013).
[114] Nesscap Energy, http://www.nesscap.com/ (accessed September 2013).
[115] Maxwell Technologies Inc., http://www.maxwell.com/ (accessed September 2013).
[116] Ioxus Inc., http://www.ioxus.com/ (accessed September 2013).
[117] M. Deschamps, E. Gilbert, P. Azais, E. Raymundo-Piñero, M. R. Ammar, P. Simon, D. Massiot, F. Béguin, *Nat. Mater.* **2013**, *12*, 351.
[118] M. Galiński, A. Lewandowski, I. Stępniak, *Electrochim. Acta* **2006**, *51*, 5567.
[119] S. P. Ong, G. Ceder, *Electrochim. Acta* **2010**, *55*, 3804.
[120] A. Brandt, S. Pohlmann, A. Varzi, A. Balducci, S. Passerini, *MRS Bull.* **2013**, *38*, 554.
[121] M. Armand, F. Endres, D. MacFarlane, H. Ohno, B. Scrosati, *Nat. Mater.* **2009**, *8*, 621.
[122] Q. T. Qu, B. Wang, L .C. Yang, Y. Shi, S. Tian, Y. P. Wu, *Electrochem. Commun.* **2008**, *10*, 1652.
[123] Q. Gao, L. Demarconnay, E. Raymundo-Piñero, F. Béguin, *Energy Environ. Sci.* **2012**, *5*, 9611.
[124] V. Khomenko, E. Raymundo-Piñero, E. Frackowiak, F. Béguin, *Appl. Phys. A: Mater. Sci. Process.* **2005**, *82*, 567.
[125] A. Burke, M. Miller, *J. Power Sources* **2011**, *196*, 514.
[126] Y. Jang, J. Jo, Y.-M. Choi, I. Kim, S.-H. Lee, D. Kim, S. M. Yoon, *Electrochim. Acta* **2013**, *102*, 240.
[127] M. Zhi, A. Manivannan, F. Meng, N. Wu, *J. Power Sources* **2012**, *208*, 345.
[128] D. Ragone, *Review of Battery Systems for Electrically Powered Vehicles* SAE Technical Paper 680453, **1968**.
[129] T. Christen, M. W. Carlen, *J. Power Sources* **2000**, *91*, 210.
[130] E. J. Cairns, P. Albertus, *Annu. Rev. Chem. Biomol. Eng.* **2010**, *1*, 299.
[131] R. Padbury, X. Zhang, *J. Power Sources* **2011**, *196*, 4436.
[132] R. F. Service, *Science* **2006**, *313*, 902.
[133] R. Kötz, M. Carlen, *Electrochim. Acta* **2000**, *45*, 2483.
[134] Idoho National Laboratory, FreedomCAR Ultracapacitor Test Manual, DOE/NE-ID-11173, **2004**.
[135] International Electrotechnical Commission, *Electric double layer capacitors for use in hybrid electric vehicles – Test methods for electrical characteristics*, IEC-62576, **2006**.
[136] International Electrotechnical Commission, *Fixed electric double layer capacitors for use in electronic equipment* in Part 2. Sectional specification - Electric double layer capacitors for power applications IEC-62391–2, **2006**.
[137] A. Burke, M. Miller, H. Zhao, *Ultracapacitors in Hybrid Vehicle Applications: Testing of New High Power Devices and Prospects for Increased Energy Density*, UCD-ITS-RR-12–06, **2012**.
[138] C. Portet, P. L. Taberna, P. Simon, E. Flahaut, *J. Power Sources* **2005**, *139*, 371.
[139] M. Uno, K. Tanaka, *IEEE Trans. Ind. Electron.* **2012**, *59*, 4704.
[140] K. G. Gallagher, S. Goebel, T. Greszler, M. Mathias, W. Oelerich, D. Eroglu, V. Srinivasan, *Energy Environ. Sci.* **2014**, *7*, 1555.
[141] Maxwell Technologies Inc., Product Comparison Matrix, http://www.maxwell.com/products/ultracapacitors/docs/maxwell_technologies_product_comparison_matrix.pdf (accessed September 2013).

[142] M. Zhi, C. Xiang, J. Li, M. Li, N. Wu, *Nanoscale* **2013**, *5*, 72.
[143] C. Zheng, W. Qian, F. Wei, *Mater. Sci. Eng., B* **2012**, *177*, 1138.
[144] G. Wang, L. Zhang, J. Zhang, *Chem. Soc. Rev.* **2012**, *41*, 797.
[145] W.-Y. Tsai, R. Lin, S. Murali, L. Li Zhang, J. K. McDonough, R. S. Ruoff, P.-L. Taberna, Y. Gogotsi, P. Simon, *Nano Energy* **2012**, *2*, 403.
[146] X. Lang, A. Hirata, T. Fujita, M. Chen, *Nat. Nanotechnol.* **2011**, *6*, 232.
[147] C. Liu, Z. Yu, D. Neff, A. Zhamu, B. Z. Jang, *Nano Lett.* **2010**, *10*, 4863.
[148] L. Hu, M. Pasta, F. L. Mantia, L. Cui, S. Jeong, H. D. Deshazer, J. W. Choi, S. M. Han, Y. Cui, *Nano Lett.* **2010**, *10*, 708.
[149] V. L. Pushparaj, M. M. Shaijumon, A. Kumar, S. Murugesan, L. Ci, R. Vajtai, R. J. Linhardt, O. Nalamasu, P. M. Ajayan, *Proc. Natl. Acad. Sci. USA* **2007**, *104*, 13574.
[150] C. Du, N. Pan, *Nanotechnology* **2006**, *17*, 5314.
[151] D. Doerffel, S. A. Sharkh, *J. Power Sources* **2006**, *155*, 395.
[152] W. Peukert, *Elektrotechnische Zeitschrift* **1897**, *20*, 20.
[153] MIT Electric Vehicle Team, A *Guide to Understanding Battery Specifications*, http://web.mit.edu/evt/summary_battery_specifications.pdf (accessed December 2013).
[154] J. Liu, J. Jiang, C. Cheng, H. Li, J. Zhang, H. Gong, H. J. Fan, *Adv. Mater.* **2011**, *23*, 2076.
[155] H. Wang, H. S. Casalongue, Y. Liang, H. Dai, *J. Am. Chem. Soc.* **2010**, *132*, 7472.
[156] J. Chmiola, G. Yushin, Y. Gogotsi, C. Portet, P. Simon, P. L. Taberna, *Science* **2006**, *313*, 1760.
[157] Y. S. Yun, S. Y. Cho, J. Shim, B. H. Kim, S. J. Chang, S. J. Baek, Y. S. Huh, Y. Tak, Y. W. Park, S. Park, H. J. Jin, *Adv. Mater.* **2013**, *25*, 1993.
[158] M. Biswal, A. Banerjee, M. S. Deo, S. Ogale, *Energy Environ. Sci.* **2013**, *6*, 1249.
[159] S. Bose, T. Kuila, A. K. Mishra, R. Rajasekar, N. H. Kim, J. H. Lee, *J. Mater. Chem.* **2012**, *22*, 767.

